TABLE 1.—Body weights, food consumptions, and DC intake in mice treated with DC after DEN initiation.

Group	Number of mice tested	Terminal body weight (g)	Food consumption (g/kg BW/day)	DC intake (g/kg BW/day)
DEN alone	8	51.1 ± 6.8	122.1 ± 16.3	0
DEN + DC	14	44.5**±3.0	119.2 ± 17.3	178.9 ± 25.9

a) Mean ± SD.
**: Significantly different from the DEN group at $p < 0.01$ (Student t-test).

and the incidence of these foci was 43% in the DEN + DC group and 38% in the DEN group. In the DEN + DC group, hepatocellular adenomas (29%) and carcinomas (14%) were also observed, and the total incidence of hepatocellular tumors was 36%; this incidence was significantly higher in this group as compared to the DEN group ($p < 0.01$). In the histochemical staining of GGT performed on frozen sections, altered foci and tumors showed positive reactions (Figure 3,

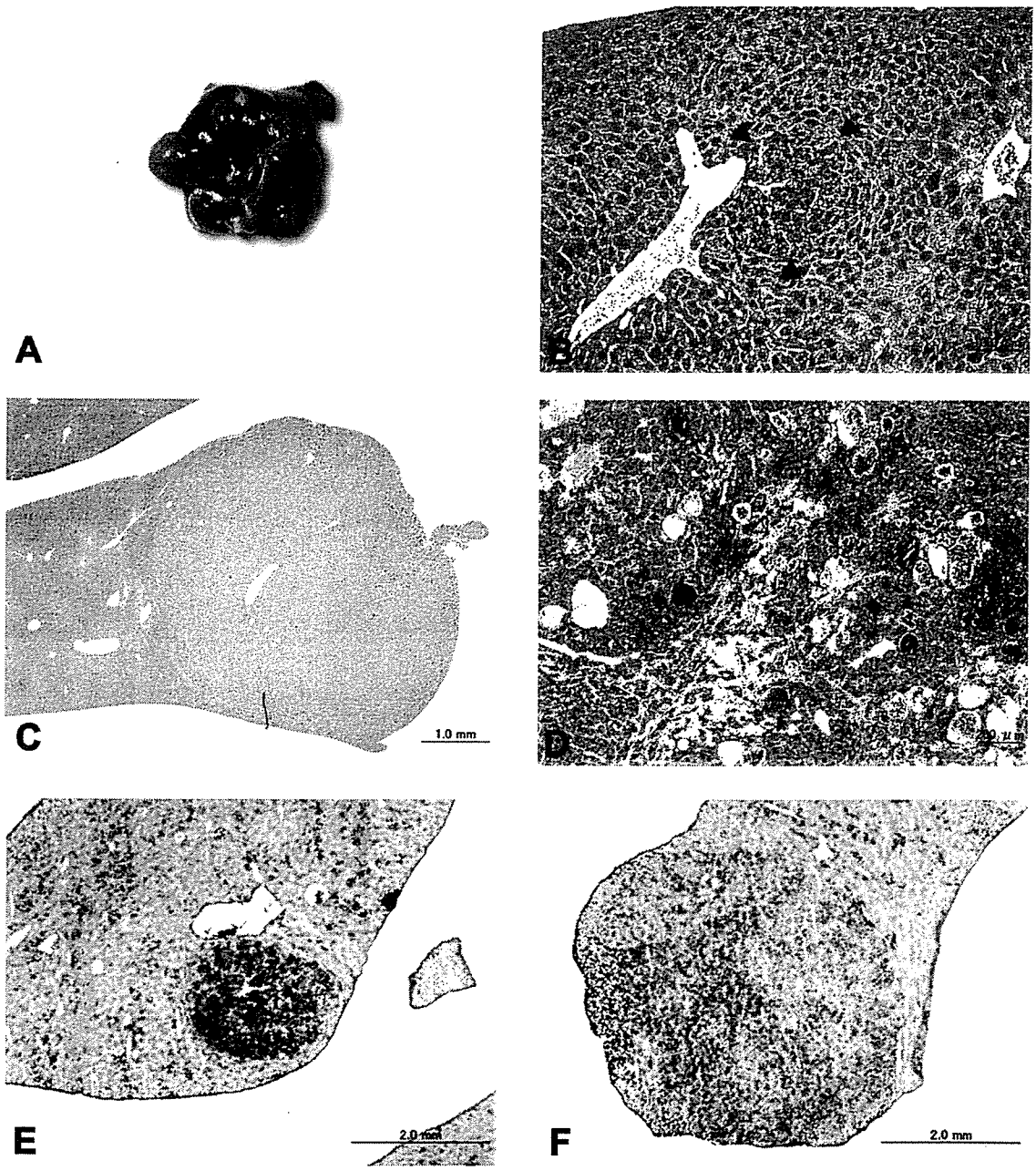

FIGURE 3.—Proliferative lesions in the livers of mice treated with DC after DEN initiation. (A) Macroscopic findings of the liver tumors in mice in the DEN + DC group. (B) Hepatocellular altered focus of a basophilic cell type (enclosed by closed triangles). (C) Hepatocellular carcinoma. Low magnification. (D) Hepatocellular carcinoma that is different from that shown in Figure 3C. Higher magnification. (E and F) Histochemical staining of GGT. GGT-positive reactions are observed in an altered focus (E) and in hepatocellular carcinoma (F).

TABLE 2.—Incidences (percentages) of proliferative lesions in the liver of mice treated with DC after DEN initiation.

Group	Number of mice tested	Altered foci	Adenom	Carcinom	Adenoma + Carcinoma
DEN alone	8	3[a)] (38)	0 (0)	0 (0)	0 (0)
DEN + DC	14	6 (43)	4 (29)	2 (14)	5 (36)**

[a)] Number of mice.
**: Significantly different from the DEN group at $p < 0.01$ (Wilcoxson test).

Table 2). Similar to other histopathological findings, centrilobular hypertrophy and necrotic foci of the hepatocytes were also observed in the DEN + DC group (data not shown).

Gene Expressions in Liver Tissues

The findings of the gene expressions by the 2 microarray analyses are shown in Table 3. A level of up- or down-regulation greater than 2-fold was observed in 11 genes (up-regulation, 8 genes; down-regulation, 3 genes) of 192 genes in two microarrays. In the stress and toxicity pathway array and the signal transduction array, significant or remarkable up-regulations were observed in the oxidative stress- and metabolism-related genes, such as *Cyp1a1*, *Hmox1*, *Cyp1a2*, and *Pgr* (sex hormone gene), in the DEN + DC group. On the other hand, *Trail* was significantly down-regulated in both arrays.

The validation of gene expression in all animals was performed by real-time RT-PCR for the genes that showed significant and remarkable fluctuations in expression in the microarray analyses (Figure 4). In addition to these genes, *Ogg1* and *Txnrd1*, which we focused on in our previous studies and which are oxidative stress-related genes, were also examined. A significant up-regulation in mean gene expression was observed in *Cyp1a1*, *Hmox1*, *Ogg1*, and *Txnrd1* in the DEN + DC group. In the same group, the mean expression of *Trail* was significantly down-regulated. In the expression analysis carried out on the individual mice in the DEN + DC group, *Trail* showed a tendency toward low levels of expression in the mice with tumors. *Ogg1* also showed a tendency toward low levels of expression in mice with tumors in the DEN + DC group, although its mean expression was significantly up-regulated as compared with its expression in the DEN group. The expression of the other genes in the present examination did not show any remarkable tendency toward either up- or down-regulation in the mice with hepatocellular tumors in the DEN + DC group.

Gene Expression Analysis in the Liver Tumor Areas

In the microarray and real-time RT-PCR analysis, *Ogg1* and *Trail* were selected. In addition to these 2 genes, *Cyp1a1* and *Txnrd1* were also examined as marker genes of oxidative stress. The results of the expressions analysis of these genes in the microdissected tumor areas of the livers of the 3 mice selected from each group are shown in Figure 5.

The mean expression of *Cyp1a1* and *Txnrd1* showed a tendency toward up-regulation in the tumor areas, and a significant up-regulation was observed in the nontumor areas in the mice in the DEN + DC group as compared to the nontumor tissues in the mice in the DEN group. The expression of *Ogg1* was not remarkably up-regulated in the tumor areas, although significant up-regulation was observed in the nontumor areas in the mice in the DEN + DC group. On the other hand, a significant down-regulation of *Trail* was observed in the tumor areas in the mice in the DEN + DC group, although the expression of *Trail* in the nontumor areas in this group was similar to that observed in the DEN group.

DISCUSSION

The histopathological examinations conducted in the present study demonstrated that DC enhanced the induction of hepatocellular tumors in mice, and these data support our previous reports that found that DC has hepatocarcinogenic potential in mice. In the special staining of GGT, the altered hepatocellular foci and tumors in the liver showed a positive

TABLE 3.—cDNA Microarray analysis of the gene expressions in the liver tissues of mice treated with DC after DEN initiation.

Gen Bank Accession No.	Description	*Symbol*	DEN alone (r = 3) Ratio	DEN alone (r = 3) S.D.	DEN + DC (r = 3) Ratio	DEN + DC (r = 3) S.D.	Classification[a)]
	Stress & Toxicity Pathway						
Up							
NM_030677	Glutathione peroxidase 2	*Gpx2*	1.00	0.31	24.09	15.94**	Oxidative and Metabolic stress
NM_009992	Cytochrome P450, family 1, subfamily a, polypeptide 1	*Cyp1a1*	1.00	0.48	16.97	5.48**	Oxidative and Metabolic stress
NM_010442	Heme oxygenase (decycling) 1	*Hmox1*	1.00	0.73	4.14	1.49**	Oxidative and Metabolic stress
NM_010231	Flavin containing monooxygenase 1	*Fmo1*	1.00	0.36	2.85	1.51	Oxidative and Metabolic stress
NM_009993	Cytochrome P450, family 1, subfamily a, polypeptide 2	*Cyp1a2*	1.00	0.32	2.32	0.52*	Oxidative and Metabolic stress
Down							
NM_009425	Tumor necrosis factor (ligand) superfamily, member 10	*Trail*	1.00	0.94	0.04	0.13*	Apoptosis signaling
NM_007836	Growth arrest and DNA (ligand) damage inducible 45 alpha	*Gadd45a*	1.00	0.24	0.48	0.33	Growth arrest and senescence
	Signal Transduction in Cancer						
Up							
NM_007742	Procollagen, type I, alpha 1	*Col1a1*	1.00	0.34	3.14	1.49	MAP kinase pathway
NM_008829	Progesterone receptor	*Pgr*	1.00	0.28	2.94	0.21**	Estrogen pathway
NM_010442	Heme oxygenase (decycling) 1	*Hmox1*	1.00	0.74	2.79	1.72	Hypoxia pathway
NM_009743	RIKEN cDNA A630035D09 gene	*Bcl2l1*	1.00	0.35	2.16	1.11	STAT pathway
Down							
NM_009425	Tumor necrosis factor (ligand) superfamily, member 10	*Trail*	1.00	0.28	0.41	0.03*	PI3/AKT pathway
NM_021283	Interleukin 4	*Il4*	1.00	0.69	0.49	0.12	STAT pathway

[a)] Classification is based on the microarray instructions.
'* or **'represent significant differences from the DEN alone group at $p < 0.05$ or 0.01, respectively (t-test).

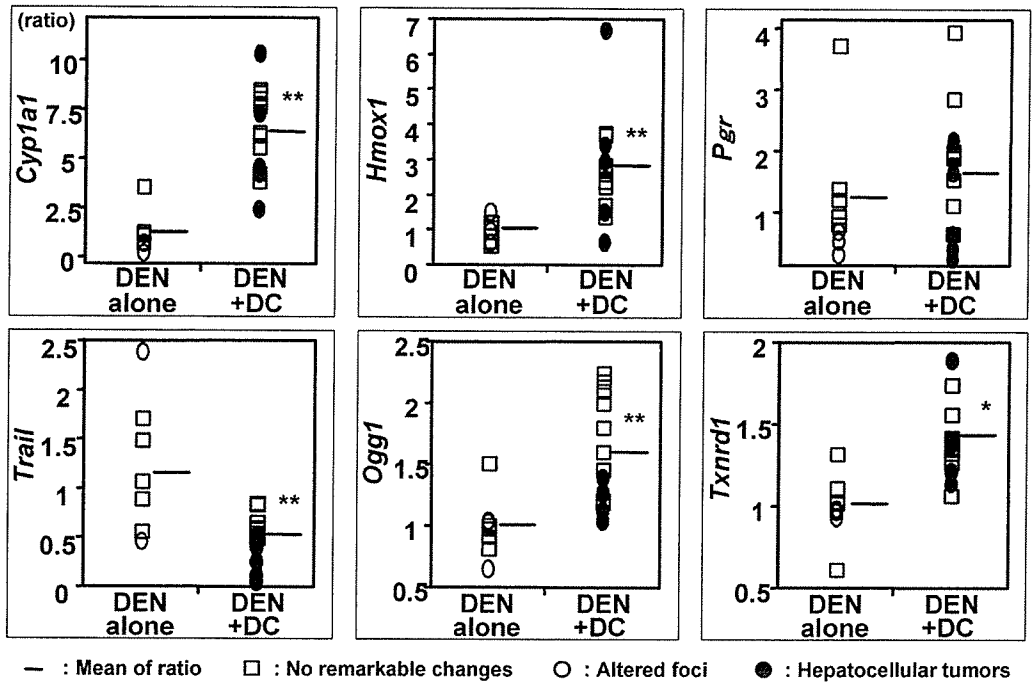

FIGURE 4.—Gene expressions in the livers of mice treated with DC after DEN initiation. Symbols represent each mouse with tumors (closed circles), altered foci (open circles), and no proliferative lesions (squares). Bars represent the mean of each group. "* or**" represent the significant difference from the DEN group at $p < 0.05$ or 0.01, respectively (t-test).

reaction. These data provide supportive evidence indicating that staining of GGT in the liver is a useful tool for the prediction of hepatocellular tumors in mice.

In gene expression analyses carried out by using microarrays in the liver tissues at the tumor formation stage, significant (or remarkable) fluctuations were observed in the expression of certain genes in the DEN + DC group. In addition to the expression of oxidative stress- and metabolism-related genes, such as *Cyp1a1*, *Homx1*, and *Cyp1a2*, significant fluctuations were observed in the expression of *Pgr* and *Trail*. Similar changes in the mean expression of *Cyp1a1*, *Homx1*, and *Trail* in the DEN + DC group were also confirmed by real-time RT-PCR analysis. In our previous study, DC also enhanced the production of reactive oxygen species (ROS) in vitro and the expression of *Cyp1a1* and *Cyp1a2* in the livers of mice at the early stage of hepatocarcinogenesis (Moto et al., 2005, 2006). It has been reported that CYP1A isoforms, such as CYP1A1 and CYP1A2, indirectly result in the production of very large amounts of oxidative stress-inducible substances, such as ROS, in comparison to other CYPs (Puntarulo and Cederbaum, 1998; Canistro et al., 2002). *Hmox1* plays an effective role in counteracting oxidative damage, and it is expected that the activation of this gene has a potential of therapeutic tool for cancer (Fabiana et al., 2004). In addition to these genes, the up-regulation of the mean expression of*Txnrd1* and *Ogg1*, which were focused on as oxidative stress-related genes in our previous studies, were also observed in the DEN + DC group. TXNRD1 plays an important role in the redox regulation of multiple intracellular processes, including DNA synthesis, transcriptional regulation, cell growth, and resistance to cytotoxic agents inducing oxidative stress (Becker et al., 2000; Nyuyen et al., 2005). Based on these results, it can be considered that oxidative stress occurs in the livers of the DC treated-mice at the tumor formation stage, and it is possible that the persistence of oxidative stress plays an important role in hepatocarcinogenesis induced by DC.

In the present gene expression analysis in the liver tissues, tendencies toward low levels of expression were observed for *Ogg1* and *Trail* in mice with hepatocellular tumors in the DEN + DC group. In fact, in the DEN group, the expression of *Ogg1* in the tumor areas was approximately equal to that in the nontumor areas of the DEN alone group; however, the expression level of this gene in the nontumor areas was significantly up-regulated in the DEN + DC group. *Ogg1*, a gene involved in the repair of 8-OHdG, is known as an indicator of oxidative DNA damage and has been shown to be potentially involved in the carcinogenesis in various experimental models (Nakae et al., 1997; Yoshida et al., 1999; Shinmura and Yokota, 2001; Kinoshita et al., 2002, 2003). Our previous study reported that the administration of DC for a period of 13 and 26 weeks increased the formation of 8-OHdG in the liver DNA of mice at the stage of preneoplastic foci formation (Moto et al., 2006). Additionally, *Cyp1a1* and *Txnrd1*, which were used as markers of oxidative stress genes in this study, were remarkably up-regulated in the tumor areas in the livers of mice in the DEN + DC group. Therefore, the present results suggest a possibility that the ability of *Ogg1* to repair the oxidative DNA damage induced by DC failed in the hepatocellular tumors in which high levels of oxidative stress occurred.

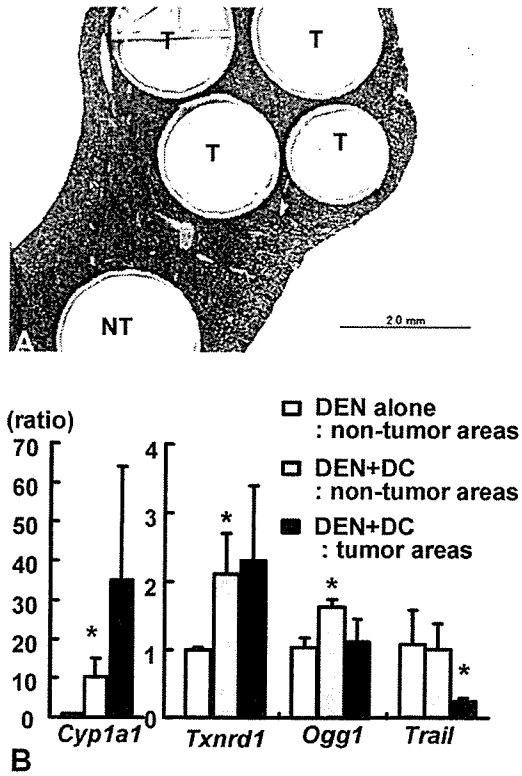

FIGURE 5.—Gene expressions in the hepatocellular tumor areas of mice treated with DC after DEN initiation. (A) Total RNA was purified from the sections microdissected from the tumor areas (T) and non-tumor areas (NT) in the frozen liver slices of the mice. (B) Gene expressions in each area. The tumor areas (closed columns) and nontumor areas (dark columns) in the DEN + DC group were collected from the liver of the same mouse. Columns represent the mean ± SD of the 3 mice. "*" represents significant difference from the DEN group at $p < 0.05$ (t-test).

A significant down-regulation in the expression of *Trail* was observed in the tumor areas in the livers of mice in the DEN + DC group. TRAIL is a member of the TNF family of cytokines that can induce apoptotic cell death in a variety of tumor tissues, and preclinical studies in mice and non-human primates have shown the potential utility of recombinant TRAIL for cancer therapy (Ashkenazi et al., 1999; Walczak et al., 1999; Yagita et al., 2004). Therefore, the down-regulation of *Trail* expression indicates the possibility that apoptosis and the self-regulation of carcinogenesis are inhibited in the tumors induced by DC. It is well recognized that one possible mechanism of nongenotoxic carcinogens is an alteration of apoptosis regulation because dysregulation of apoptosis results in the decreasing ability of cells to undergo apoptosis. For example, phenobarbital (PB) and WY-14643, representative nongenotoxic carcinogens in mice and rats, gradually increase anti-apoptosis proteins during the hepatocarcinogenesis in mice (Christensten et al., 1999). Additionally, it has been reported that short-term treatments of PB showed no increase of apoptosis in the liver of mice (Bursch et al., 2002). In our previous study, the down-regulation of *Trail* expression was not observed in our 2- and 7-week studies of DC. Taking these data into account, it is speculated that *Trail* plays an important role at the later stages of carcinogenesis, such as in the stages of promotion or progression, in the DC-induced hepatocarcinogenicity.

In conclusion, the present investigation on the gene expressions in the hepatocellular tumors induced by DC in a 2-stage hepatocarcinogenesis model of mice have demonstrated the possibility that oxidative stress, failure of the ability to repair oxidative DNA damage, and the inhibition of apoptosis occur in the tumor areas. In addition, the results of our previous and present studies suggest that the continuous treatment of DC induces oxidative stress in the liver and hepatocellular tumors, and oxidative stress plays an important role in the DC-induced hepatocarcinogenesis in mice.

ACKNOWLEDGMENTS

We are grateful to Novartis Animal Health Inc. for supplying DC. This work was supported in part by a grant-in-aid for research on the safety of veterinary drug residues in food of animal origin from the Ministry of Health, Labour and Welfare of Japan (H16-shokuhin-006).

REFERENCES

Ashkenazi, A., Pai, R. C., Fong, S., Leung, S., Lawrence, D. A., Marsters, S. A., Blackie, C., Chang, L., McMurtrey, A. E., Herbert, A., DeForge, L., Koumenis, I. L., Lewis, D., Harris, L., Bussiere, J., Koppen, H., Shahrokh, Z., and Schwall, R. H. (1999). Safety and antitumor activity of recombinant soluble Apo2 ligand. *J Clin Invest* **104**, 155–62.

Becker, K., Gromer, S., Schirmer, R. H., and Muller, S. (2000). Thioredoxin reductase as a pathophysiological factor and drug target. *Eur J Biochem* **267**, 6118–25.

Bursch, W., Wastl, U., Hufnagl, K., and Schulte-Hermann, R. (2002). No increase of apoptosis in regressing mouse liver after withdrawal of growth stimuli or food restriction. *Toxicol Sci* **85**, 507–514.

Canistro, D., Cantelli-Forti, G., Biagi, G. L., and Palini, M. (2002). Re: Dioxin increases reactive oxygen production in mouse liver mitochondria. *Toxicol Appl Pharmacol* **185**, 74–5.

Carter, K. C., Gandolfi, A. J., and Sipes, I. G. (1985). Characterization of dimethylnitrosamine -induced focal nodular lesions in the livers of new born mice. *Toxicol Pathol* **13**, 3–9.

Christensen, J. G., Romach, E. H., Healy, L. N., Gonzales, A. J., Anderson, S. P., Malarkey, D. E., Corton, J. C., Fox ,T. R., Cattley, R. C., and Goldsworthy, T. L. (1999). Altered bcl-2 family expression during non-genotoxic hepatocarcinogenesis in mice. *Carcinogenesis* **20**, 1583–90.

Dybdahl, M., Risom, L., Moller, P., Autrup, H., Wallin, H., Vogel, U., Bornholdt, J., Daneshvar, B., Dragsted, L. O., Weimann, A., Poulsen, H. E., and Loft, S. (2003). DNA adduct formation and oxidative stress in colon and liver of Big Blue rats after dietary exposure to diesel particles. *Carcinogenesis* **24**, 1759–66.

Fabiana, C., Roberto, M., Alejandra G., Alcira B., and Elba, V. (2004). Immunohistochemical analysis of heme oxygenase-1 in preneoplastic and neoplastic lesions during chemical hepatocarcinogenesis. *Int J Exp Pathol* **85**, 213–22.

Fortini, P., Pascucci, B., Parlanti, E., D'Errico, M., Simonelli, V., and Dogliotti, E., (2003). 8-Oxoguanine DNA damage: at the crossroad of alternative repair pathways. *Mutat Res* **531**, 127–39.

Kasai, H. (1997). Analysis of a form of oxidative DNA damage, 8-hydroxy-2′-deoxyguanosine, as a marker of cellular oxidative stress during carcinogenesis.*Mutat Res* **387**, 147–63.

Kinoshita, A., Wanibuchi, H., Imaoka, S., Ogawa, M., Matsuda, C., Morimura, K., Funae, Y., and Fukushima, S. (2002). Formation of 8-hydroxydeoxyguanosin and cell-cycle arrest in the rat liver via generation of oxidative stress by phenobarbital: association with expression profiles of $p21^{WAF1/Cip1}$, cyclin D1 and Ogg1. *Carcinogenesis* **23**, 341–49.

Kinoshita, A., Wanibuchi, H., Morimura, K., Wei, M., Shen, J., Imaoka, S., Funae, Y., and Fukushima, S. (2003). Phenobarbital at low dose exerts hormesis in rat hepatocarcinogenesis by reducing oxidative DNA damage, altering cell proliferation, apoptosis and gene expression. *Carcinogenesis* **24**, 1389–99.

Lee, G. H., Nomura, K., and Kitagawa, T. (1989). Comparative study of diethylnitrosoamine-initiated two-stage hepatocarcinogenesis in C3H, B57BL and BALB mice promoted by various hepatopromoters. *Carcinogenesis* **12**, 2227–30.

Michael, R., Emmert-Buck, R. F., Bonner, P. D., Smith, R. F., Chuaqui, Z., Zhuang, S. R., Goldstein, R. A., and Weiss, L. A. (1996). Laser capture microdissection. *Science* **274**, 998–1001.

Moto, M., Okamura, M., Muto, T., Kashida, Y., Machida, N., and Mitsumori, K. (2005). Molecular pathological analysis on the mechanism of liver carcinogenesis in dicyclanil-treated mice. *Toxicology* **207**, 419–36.

Moto, M., Umemura, T., Okamura, M., Muguruma, M., Ito, T., Jin, M., Kashida, Y., and Mitsumori, K. (2006). Possible involvement of oxidative stress in dicyclanil-induced hepatocarcinogenesis in mice. *Arch Toxicol* **204**, *in press*.

Nakae, D., Kobayashi, Y., Akai, H., Andoh, N., Satoh, H., Ohashi, K., Tsutsumi, M., and Konishi, Y. (1997). Involvement of 8-hydroxyguanine formation in the initiation of rat liver carcinogenesis by low dose levels of *N*-nitrosodiethylamine. *Cancer Res* **57**, 1281–87.

Nguyen, P., Awwad, R. T., Smart, D. D., Spitz, D. R., and Gius, D. (2006). Thioredoxin reductase as a novel molecular target for cancer therapy. *Cancer Lett* **236**, 164–174.

Porta, G. D., Dragani, T. A., and Manenti, G. (1987). Two-stage liver carcinogenesis in the mouse. *Toxicol Pathol* **15**, 299–34.

Puntarulo, S., and Cederbaum, A. I. (1998). Production of reactive oxygen species by microsomes enriched in specific human cytochrome P450 enzymes. *Free Radic Biol Med* **24**, 1324–30.

Shinmura, K., and Yokota, J. (2001). The OGG1 gene encodes a repair enzyme for oxidatively damaged DNA and is involved in human carcinogenesis. *Antioxid Redox Signal* **3**, 597–609.

Suarez-Quian, C. A., Goldstein, S. R., Pohida, T., Smith, P. D., Peterson, J. I., Wellner, E., Ghany, M., and Bonner, R. F. (1999). Laser capture microdissection of single cells from complex tissues. *Biotechniques*, **26**, 328–35.

Umemura, T., Takagi, A., Sai, K., Hasegawa, R., and Kurokawa, Y. (1998). Oxidative DNA damage and cell proliferation in kidneys of male and female rats during 13-weeks exposure to potassium bromate ($KBrO_3$). *Arch Toxicol* **72**, 264–69.

Walczak, H., Miller, R. E., Ariail, K., Gliniak, B., Griffith, T. S., Kubin, M., Chin, W., Jones, J., Woodward, A., Le, T., Smith, C., Smolak, P., Goodwin, R. G., Rauch, C. T., Schuh, J. C., and Lynch, D. H. (1999). Tumoricidal activity of tumor necrosis factor-related apoptosis-inducing ligand in vivo. *Nat Med* **5**, 157–63.

WHO (2000). Toxicological Evaluation of Certain Veterinary Drug Residues in Food, Fifty-fourth meeting of the Joint FAO/WHO Expert Committee on Food Additives. WHO Food Additive Series 45, pp. 75–89, International Programme on Chemical Safety World Health Organization, Geneva.

Yagita, H., Takeda, K., Hayakwa, Y., Smith, M. J., and Okumura, K. (2004). TRAIL and its receptors as targets for cancer therapy. *Cancer Sci* **95**, 777–83.

Yoshida, M., Miyajima, K., Shiraki, K., Ando, J., Kudoh, K., Nakae, D., Takahashi, M., and Maekawa, A. (1999). Hepatotoxicity and consequently increased cell proliferation are associated with flumequine hepatocarcinogenesis in mice. *Cancer Lett* **141**, 99–107.

Volume 52(7): 903–913, 2004
Journal of Histochemistry & Cytochemistry
http://www.jhc.org

ARTICLE

Microdissected Region-specific Gene Expression Analysis with Methacarn-fixed, Paraffin-embedded Tissues by Real-time RT-PCR

Hironori Takagi, Makoto Shibutani, Natsumi Kato, Haruka Fujita, Kyoung-Youl Lee, Shu Takigami, Kunitoshi Mitsumori, and Masao Hirose

Division of Pathology (HT,MS,NK,HF,K-YL,ST,MH), National Institute of Health Sciences, Tokyo; United Graduate School of Veterinary Sciences (HT,MS,KM), Gifu University, Gifu; and Laboratory of Veterinary Pathology (KM), Tokyo University of Agriculture and Technology, Tokyo, Japan

SUMMARY We have previously shown methacarn to be a versatile fixative for analysis of proteins, DNA, and RNA in paraffin-embedded tissues (PETs). In this study we analyzed its suitability for quantitative mRNA expression analysis of microdissected PET specimens using a real-time RT-PCR technique. Fidelity of expression in the methacarn-fixed PET sections, with reference to dose-dependent induction of cytochrome P450 2B1 in the phenobarbital-treated rat liver, was high in comparison with the unfixed frozen tissue case, even after hematoxylin staining. RNA yield from methacarn-fixed PET sections was equivalent to that in unfixed cryosections and was also not significantly affected by hematoxylin staining. Correlations between the expression levels of target genes and input amounts of extracted RNA in the range of 1–1000 pg were very high (correlation coefficients >0.98), the regression curves being similar to those with unfixed cryosections. Although cell numbers should be optimized for each target gene/tissue, ≥200 cells were necessary for accurate measurement in 10-μm-thick rat liver sections judging from the variation of measured value in small microdissected areas. These results indicate high performance with methacarn, close to that of unfixed tissues, regarding quantitative expression analysis of mRNAs in microdissected PET-specimens. (J Histochem Cytochem 52:903–913, 2004)

KEY WORDS
methacarn
paraffin-embedded tissue
mRNA expression
real-time RT-PCR
microdissection
hematoxylin staining

THE RECENT DEVELOPMENT of microdissection techniques has enabled us to perform biochemical or molecular biological analyses of small tissue areas (Emmert-Buck et al. 1996; Schütze and Lahr 1998). For this purpose, use of cryosections from unfixed frozen tissues has become the gold standard because molecules to be analyzed remain intact. However, preparation of cryosections from unfixed frozen tissue for the purpose of microdissection may not be optimal for routine samples because of the inconvenience in terms of tissue storage and the skill required for preparation and subsequent microdissection. Therefore, tissue embedding after fixation is preferable for microdissected tissue preparations if high yield and quality of molecules can be guaranteed.

For histological assessment, tissue fixation and subsequent paraffin embedding are routinely employed because of the ease of handling tissues and subsequent staining, as well as the good preservation of morphology. Usually, formaldehyde-based fixatives, such as buffered formalin, are used for this purpose. However, with such crosslinking agents there is limited performance in terms of the yield and quality of extracted RNA (reviewed by Srinivasan et al. 2002), protein (Ikeda et al. 1998; Shibutani et al. 2000), and genomic DNA (Srinivasan et al. 2002), with consequent difficulty in the analysis of microdissected, histologically defined tissue areas. Extraction efficiency and quality of molecules are critical for analysis in microdissected cells. Recently, we found that methacarn, a non-crosslinking organic solvent fixative (Puchtler et al. 1970), meets critical criteria for analysis of RNAs, proteins,

Correspondence to: Dr. M. Shibutani, Div. of Pathology, National Institute of Health Sciences, 1-18-1 Kamiyoga, Setagaya-ku, Tokyo 158-8501, Japan. E-mail: shibutan@nihs.go.jp
Received for publication December 3, 2003; accepted March 9, 2004 [DOI: 10.1369/jhc.3A6215.2004].

0022-1554/04/$3.30

and DNAs in microdissected defined areas of paraffin-embedded tissue (PET) sections by simple extraction protocols (Shibutani et al. 2000; Shibutani and Uneyama 2002; Uneyama et al. 2002). With regard to RNA expression analysis using RT-PCR, long RNA fragments as well as rare RNA species can successfully be amplified from methacarn-fixed PET sections (Shibutani et al. 2000).

For RNA expression analysis in microdissected tissue samples, PCR-based techniques are suitable because of their sensitivity with samples having as few as 10 copies of a specific transcript. In this study we examined the suitability of methacarn fixation for measurement of mRNA expression levels in microdissected PET specimens using real-time PCR (Higuchi et al. 1992,1993). For this purpose, we assessed (a) fidelity of mRNA expression in comparison with unfixed frozen tissue, (b) abundance of amplifiable mRNAs in comparison with unfixed cryosections, (c) linearity between the input amount of extracted total RNA and the expression level, (d) effect of tissue staining with hematoxylin, and (e) cell numbers required for practical measurement of mRNA expression in hematoxylin-stained tissue.

Materials and Methods

Animals and Experimental Design

Sprague–Dawley rats from Charles River Japan (Kanagawa, Japan) were used. They were maintained in an air-conditioned animal room (temperature 24 ± 1C; relative humidity 55 ± 5%) with a 12-hr light/dark cycle and allowed ad libitum access to feed and tap water. All animals, including pregnant rats, were housed individually in polycarbonate cages with wood chip bedding.

To measure the dose-dependent induction of cytochrome P450 (CYP) 2B1 mRNA in the liver by treatment with sodium phenobarbital (PB; Wako Pure Chemical Industries, Osaka, Japan), female rats received daily IP injections of PB at doses of 0 (vehicle saline), 1.25, 5, 20, or 80 mg/kg body weight/day for 3 days and were sacrificed 24 hr after the last injection. The highest dose was selected according to the PB-specific enzyme induction protocol described by Kocarek et al. (1998). For practical assessment in microdissected areas, region-specific expression of mRNAs was measured in the hypothalamic medial preoptic area (MPOA) in male and female pups at postnatal day 10, the time point for the late stage of brain sexual differentiation in rats (Rhees et al. 1990a,b).

All animals used in the present study were sacrificed by exsanguination from the abdominal aorta under ether anesthesia. The animal protocols were reviewed and approved by the Animal Care and Use Committee of the National Institute of Health Sciences, Japan.

Tissue Fixation

Methacarn solution consisting of 60% (v/v) absolute methanol, 30% chloroform, and 10% glacial acetic acid was freshly prepared before fixation and stored at 4C until use. At autopsy, livers were removed and 3-mm-thick slices or 5 × 5 × 3 mm-sized tissue blocks were prepared from the left lateral lobe and fixed in methacarn for 2 hr at 4C with gentle agitation. Whole brains of rat pups were also removed and subjected to methacarn fixation. For embedding, liver slices/blocks and coronal brain slices, including the hypothalamus, were dehydrated three times for 1 hr in fresh 99.5% ethanol at 4C, immersed in xylene for 1 hr and then three times for 30 min at room temperature (RT), and immersed in hot paraffin (60C) four times for 1 hr, for a total of 4 hr. Embedded tissues were stored at 4C for up to 6 months until tissue sectioning. Unfixed liver tissue samples, either 3 × 3 × 1 mm or 5 × 5 × 3 mm, were also prepared from portions adjacent to the tissue samples for methacarn fixation and immersed in RNAlater (Ambion; Austin, TX) overnight at 4C, or embedded in Tissue-Tek 4583 OCT compound (Sakura Finetek Japan; Tokyo, Japan) by quick freezing on dry ice. They were stored at −80C until direct extraction of RNA or sectioning before RNA extraction, respectively. For immunohistochemical analysis of MPOA in pups, brains were immersed in 10% neutral buffered formalin (pH 7.4) overnight at RT with gentle agitation. Coronal brain slices that included the hypothalamus were then routinely embedded in paraffin.

Preparation of Tissue Specimens and Microdissection

For assessment of dose-dependent induction of CYP2B1 in the rat liver by PB treatment, methacarn-fixed PETs were sectioned at 10 μm and mounted on 2.5-μm PEN-foil film (Leica Microsystems; Tokyo, Japan) overlaid on a glass slide that had been treated with 3% H_2O_2 for 10 min, rinsed with absolute ethanol, and then dried in an incubator overnight at 37C. The sections were deparaffinized by immersion in xylene twice for 2 min, followed by 99.5% ethanol once for 30 sec. Sections were either unstained or stained with Tissue Tek Hematoxylin 3G (Sakura Finetek Japan) for 10 sec, rinsed briefly with water, and air-dried. For assessment of linearity between the input amounts of total RNA and expression levels of target genes, as well as for estimation of the relative abundance of amplifiable mRNAs, series of 20 10-μm-thick sections were prepared from 5 × 5 × 3-mm unfixed frozen tissues and methacarn-fixed PETs and were collected into 1.5-ml tubes. Integrity of extracted total RNA was also examined in these preparations by judging the resolution of rRNAs in agarose gel. In this experiment, effect of fixation itself on the integrity was also examined with fresh-frozen sections fixed with methacarn for 10 min at 4C. For preparation of tissue sections and hematoxylin staining, RNase-free ultrapure water, prefiltrated with a Gengard filter attached to an Elix 3 ultrapure water system (Millipore; Billerica, MA) was employed. Whole tissue areas of methacarn-fixed PET sections were dissected together with PEN-foil film and collected into 1.5-ml tubes for the dose-dependent expression analysis. With microdissected small tissue areas, hematoxylin-stained 10-μm-thick sections were used and circles of 30-, 50-, and 100-μm radius were microdissected from mid-zonal areas of hepatic lobules using PALM Robot-MicroBeam equipment (Carl Zeiss; Tokyo, Japan). In addition, for assessment of the relationship between the cell number and the amount of extracted total RNA, square ar-

eas of 250 × 250, 500 × 500, and 1000 × 1000 μm were also microdissected.

For microdissection of MPOA, 6-μm-thick sections between pairs of 20-μm-thick sections were prepared from methacarn-fixed rat brain PETs. The 20-μm sections were mounted on PEN-foil film. As shown in Figure 1, localization of the sexually dimorphic nucleus of the preoptic area (SDN-POA), identified as an intensely stained cellular region, was determined under microscopic observation of 6-μm-thick sections stained with hematoxylin and eosin, and the bilateral portions of the MPOA (1000 × 600 μm) containing SDN-POA were microdissected from the adjacent unstained 20-μm-thick sections. Because of sexual dimorphism in the volume of SDN-POA, six to ten sections in males and four to six sections in females were used for microdissection.

RNA Extraction

Quantitative mRNA expression analysis of target genes was performed with a real-time RT-PCR system. In cases of unfixed frozen liver tissue blocks (3 × 3 × 1 mm), whole tissue sections of liver PETs, and microdissected MPOAs from the brain PET sections, total RNA was extracted using RNA STAT-60 (Tel-Test "B"; Friendswood, TX), precipitated with isopropanol in the presence of 2 μg/ml glycogen as a carrier, and reconstituted with 10 μl of ultrapure water treated with diethylpyrocarbonate (Ambion). Unfixed frozen tissue blocks were disintegrated in RNA STAT-60 solution with a Mixer Mill MM300 (QIAGEN; Tokyo, Japan) before extraction. For liver tissue sections of 5 × 5 mm from 5 × 5 × 3-mm unfixed frozen tissues and methacarn-fixed PETs, total RNA was extracted with RNeasy Mini (QIAGEN) according to the manufacturer's protocol, and the final elution volume was set at 30 μl. Contaminating genomic DNA was digested with DNase I (Ambion) at the end of the extraction according to the manufacturer's protocol. One μl of isolated RNA was labeled with a RiboGreen RNA Quantitation kit (Molecular Probes; Eugene, Oregon) and concentrations were estimated with a fluorescence spectrophotometer F2500 (Hitachi; Tokyo, Japan) in 1 ml of total volume with water.

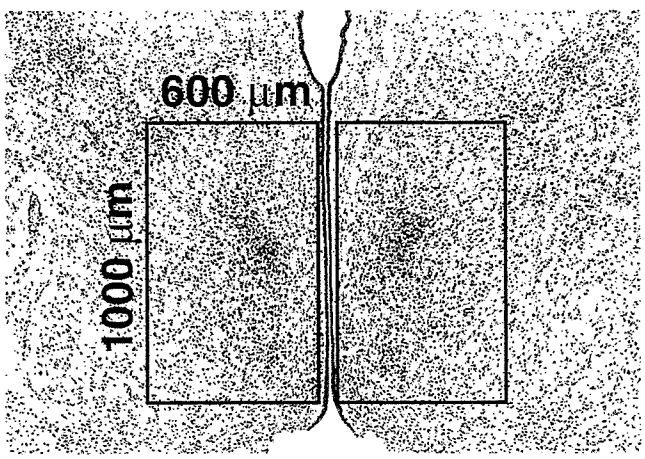

Figure 1 The microdissected area for expression analysis in the MPOA of rat pups at postnatal day 10. The intensely stained cellular regions near the center of each rectangle area are SDN-POAs.

In cases of small tissue areas microdissected from liver PET sections, RNAqueous-Micro (Ambion) was used for total RNA extraction and the final elution volume was set at 20 μl. Contaminating genomic DNA was digested with DNase I included in the kit and the final volume was set to be 25.3 μl.

Real-time RT-PCR

When two-step real-time RT-PCR was planned, RT was performed using 1 μl (200 U) of SuperScript II RNase H⁻ Reverse Transcriptase with 2 μl of 50 μg/ml random hexamers, 1 μl of 10 mM dNTP mix, 2 μl of 10 × PCR buffer, 1.2 μl of 50 mM $MgCl_2$, 2 μl of 0.1 M dithiothreitol, 1 μl of RNase inhibitor, and 9.8 μl of RNA solution in a 20-μl total reaction volume (all reagents were purchased from Invitrogen; Carlsbad, CA). After treatment with 1 μl of RNase H, 1 μl of RT product was subjected to real-time PCR in a 25 μl of total reaction volume with the ABI PRISM 7700 Sequence Detection System (Applied Biosystems Japan; Tokyo, Japan) using either QuantiTect SYBR Green PCR Kit (QIAGEN) or TaqMan Universal PCR Master Mix (Applied Biosystems Japan). With this two-step RT-PCR, mRNA expression levels of CYP2B1, estrogen receptor (ER)α, ERβ, γ-aminobutyric acid transporter type 1 (GAT-1), and glyceraldehyde-3-phosphate dehydrogenase (GAPDH) were measured. Primer Express software (Version 2.0; Applied Biosystems Japan) was used for the design of primer sequences and TaqMan probes. For expression analysis of GAPDH, either SYBR Green or TaqMan probe system was applied. In the latter case, TaqMan Rodent GAPDH Control Reagents (Applied Biosystems Japan) were used. The sequences of primers and probes are listed in Table 1.

With the SYBR Green detection system, mRNA levels of CYP2B1, ERβ, GAT-1, and GAPDH were measured (1 μl of RT product, 12.5 μl of 2 × QuantiTect SYBR Green PCR Master Mix, and 300 nM of primers in a 25-μl total reaction volume). Cycle parameters in this system were as follows: initial activation at 95C for 15 min; 50 cycles of 15 sec at 94C, 30 sec for annealing, and 30 sec at 72C. Annealing temperatures for CYP2B1, ERβ, GAT-1, and GAPDH were 53C, 54C, 54C, and 59C, respectively. With the TaqMan probe detection system, mRNA levels of ERα and GAPDH were measured (1 μl of RT product, 12.5 μl of 2 × TaqMan Universal PCR Master Mix, 900 nM of primers, and 250 nM of TaqMan probe in a 25-μl total reaction volume). Cycle parameters with this system for both genes were: single step of 50C for 2 min, initial activation at 95C for 10 min; 50 cycles of 15 sec at 95C and 60 sec at 60C.

When RT and following real-time PCR were intended to be performed sequentially in one tube, one-step kits, such as the QuantiTect SYBR Green RT-PCR Kit (QIAGEN; for CYP2B1) and the QuantiTect Probe RT-PCR Kit (QIAGEN; for GAPDH) were used with 5 μl of total RNA in a 50-μl total reaction volume according to the manufacturer's protocols. Cycle parameters for CYP2B1 were similar to the above described two-step case, and a RT step at 50C for 30 min was preceded for the initial activation step at 95C for 10 min. In the case of GAPDH, cycle parameters were as follows: single step of 50C for 30 min; single step of 95C for 15 min; and 50 cycles of 94C for 15 sec followed by 60C for 60 sec.

Table 1 Sequences of primers and probes used for real-time RT-PCR

Gene	Accession No.		Sequence	Product size
CYP2B1	M37134	Sense	5′-TTGGCTCCCAAGGACATTG-3′	72 bp
		Antisense	5′-GATCTGGTACGTTGGAGGTATTTTTC-3′	
ERα	Y00102	Sense	5′-GGGCTTCCCCAACACCAT-3′	65 bp
		Antisense	5′-CGTTTCAGGGATTCGCAGAA-3′	
		Probe	5′-TGAGAACTCCCAGGCTCCCCACAA-3′	
ERβ	U57439	Sense	5′-TGCTGGATGGAGGTGCTAATG-3′	82 bp
		Antisense	5′-CGAGGTCGGGAGCGAAA-3′	
GAT-1	NM_024371	Sense	5′-CCTCTGAGATGTTTGGCAAGAA-3′	82 bp
		Antisense	5′-AATTGTACGACCCTTAACGTTGTG-3′	
GAPDH[a]	M17701	Sense	5′-GGCCGAGGGCCCACTA-3′	88 bp
		Antisense	5′-TGTTGAAGTCACAGGAGACAACCT-3′	

[a]For TaqMan PCR, a commercially available TaqMan Rodent GAPDH Control Reagents (Applied Biosystems) was used (sequence information is not available).

As a negative control for RT, reverse transcriptase (−) mock RT samples were included in each PCR experiment.

Immunohistochemical Analysis

Because ERα mRNA is differentially expressed in the MPOA depending on the gender, the corresponding protein expression was also examined immunohistochemically. A series of five 3-μm-thick sections were prepared at 30-μm intervals through the MPOA and the first of each series was stained with hematoxylin and eosin. These sections were examined microscopically and one showing the maximum size of SDN-POA was identified and selected for IHC with ERα in each animal. Deparaffinized and hydrated sections were treated with microwaving for 9 min in 0.01 M citrate buffer (pH 6.0) and treated with 1% periodic acid solution for 10 min. After incubation with mouse anti-ERα monoclonal antibody (Novocastra Laboratories, Newcastle upon Tyne, UK; × 40 dilution), immunodetection was performed using a VECTASTAIN Elite ABC KIT (Vector Laboratories; Burlingame, CA) with a standard protocol using diaminobenzidine as chromogen. The sections were then counterstained with hematoxylin. Digital photomicrographs at a magnification of ×180 were taken with a Fujix Digital Camera system (Fujifilm; Tokyo, Japan), and the numbers of immunostained nuclei within the MPOA (600 × 1000-μm areas) were counted using MacSCOPE (version 2.65; Mitani, Fukui, Japan).

Statistical Analysis

Comparison of data of mRNA expression levels and ERα-immunoreactive cell numbers in MPOA was performed with the Student's *t*-test after confirmation of equal variance of values. Pearson's correlation coefficients were calculated between the input amounts of RNA and the target gene expression levels in the validation studies in the liver and MPOA. Variability was expressed as coefficient of variation (CV).

Results

Integrity of Total RNA

Figure 2 shows the integrity of extracted total RNA from methacarn-fixed PET sections. Judging from the resolution of 18S and 28S rRNAs, integrity of total RNA was well preserved in the methacarn-fixed frozen sections (Figure 2, Lane 2) similar to that from unfixed frozen sections (Figure 2, Lane 1). In the methacarn-fixed PET sections (Figure 2, Lane 3), integrity of both rRNA bands was largely retained, but slight reduction of the band intensity of 28S rRNA was also observed as well as a slight increase of background smearing at the position below the 28S band.

Fidelity of mRNA Expression

Figure 3 shows data for mRNA expression in unfixed frozen tissue and methacarn-fixed PET sections, unstained or stained with hematoxylin. Dose-dependent induction of CYP2B1 mRNA was evident in the livers of rats treated with PB for 3 days. In the unfixed tissue, a clear dose-dependent induction of CYP2B1 was detected, and expression levels relative to that at 80 mg/kg PB were 27.5, 4.95, 1.10, and 0.33%, at 20, 5, 1.25, and 0 mg/kg, respectively. Similar dose-dependent expression was observed in the methacarn-fixed

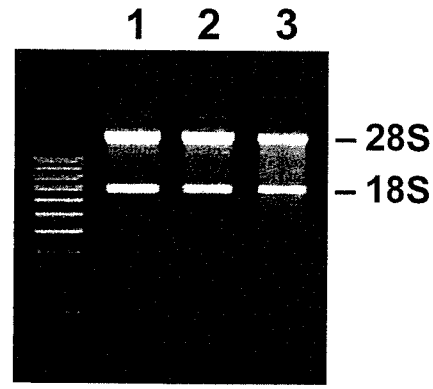

Figure 2 Integrity of total RNA extracted from methacarn-fixed rat liver PET sections. One-μg total RNA samples were resolved in a 1.0% agarose gel and visualized with ethidium bromide. Lane 1, unfixed frozen sections; Lane 2, methacarn-fixed frozen sections; Lane 3, methacarn-fixed PET sections.

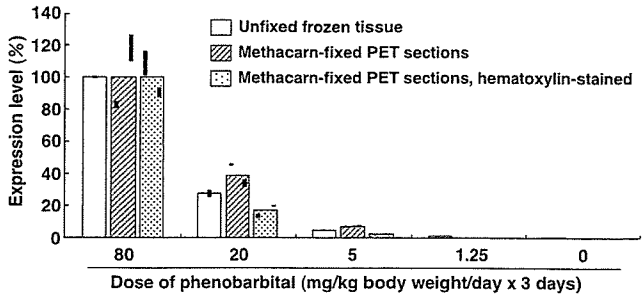

Figure 3 Comparison of gene expression pattern between the unfixed frozen tissue and stained or unstained methacarn-fixed PET sections. For analysis of dose-dependent CYP2B1 expression in the rat liver by PB, one animal was examined at each dose, and therefore the tissue source was set to be identical between preparations at each dose level. In the unfixed frozen tissue, RT was performed with 2 μg of total RNA. For methacarn-fixed PET sections, RT was performed with 335 ng of total RNA. Real-time PCR was performed in duplicate on each RT product. The upper and lower ends of the bars on each column of the graph represent the expression levels measured in duplicate from the same cDNA template.

PET sections irrespective of staining with hematoxylin, although slight suppression was noted at doses of 1.25 and 0 mg/kg. With regard to variability, there was a maximal 47% difference between the values in each RT sample at 80 mg/kg PB (unstained sections). The relative expression levels at 20, 5, 1.25, and 0 mg/kg PB were 38.6, 7.27, 0.21, and 0.06% in unstained sections and 18.1, 2.49, 0.01, and 0.02 in hematoxylin-stained sections, respectively. Reverse transcriptase (−) mock RT samples did not show any amplification on the PCR.

Relative Abundance of Amplifiable mRNA Molecules

To examine the relative abundance of amplifiable mRNA molecules in the methacarn-fixed PET sections, gene expression levels were compared with those in unfixed cryosections using liver of a rat treated with PB at 80 mg/kg body weight/day for 3 days. RNA yields from unfixed cryosections and methacarn-fixed PET sections were determined to be 35.4 ± 11.3, and 42.1 ± 6.0 ng/mm^2 area in 10-μm-thick sections, respectively (n=5). With extracted total RNAs in the range of 1–1000 pg, relative expression of CYP2B1 and GAPDH was determined (Table 2). Although expression signals for both genes could be detected with 1 pg total RNA, values varied when input amount of total RNA was decreased in both tissue section preparations. With 100 and 1000 pg of total RNA, variability of expression data, as judged by the values of CV, was reduced in both unfixed and methacarn-fixed PET sections, with a small reduction of amplifiable mRNAs for both genes in the latter compared with unfixed cryosections (88.2~98.5% for CYP2B1 with statistical difference of $p<0.05$ at 100 pg; 76.5~86.3% for GAPDH with $p<0.05$ at 1000 pg).

Linearity Assessment of mRNA Expression with Input Amount of Total RNA

Figure 4 shows comparisons of regression curves between cryosections and methacarn-fixed PET sections from the liver of a PB-treated rat, based on the data shown in Table 2. In the methacarn-fixed PET sections, the linearity between input amounts of total RNA and expression levels was very high for both CYP2B1 and GAPDH genes and the curves were almost identical with those for unfixed sections. The correlation coefficients in the analysis of CYP2B1 and GAPDH with unfixed frozen sections were 0.997 and 0.990, respectively. Similarly, correlation coefficients in the methacarn-fixed PET sections were 0.991 and 0.982, respectively.

Variability of the mRNA expression data during the processes of RT and after real-time PCR was assessed for four genes with the same RNA sample de-

Table 2 Relative abundance of amplifiable mRNAs in methacarn-fixed PET sections[a]

	No. of samples	Extracted total RNA (pg)			
		1000	100	10	1
CYP2B1					
Unfixed cryosections	5	100.0 ± 7.1[b]	8.08 ± 0.41	0.61 ± 0.10	0.12 ± 0.04
		(7.1)[c]	(5.1)	(16.4)	(33.3)
Methacarn-fixed PET sections	5	98.5 ± 12.4	7.13 ± 0.69[d]	0.64 ± 0.09	0.10 ± 0.04
		(12.6)	(9.7)	(14.1)	(40.0)
GAPDH					
Unfixed cryosections	5	100.0 ± 13.3	8.54 ± 0.46	0.79 ± 0.15	0.06 ± 0.04
		(13.3)	(5.4)	(19.0)	(66.7)
Methacarn-fixed PET sections	5	76.5 ± 13.6[d]	7.37 ± 1.10	0.83 ± 0.37	0.04 ± 0.03
		(17.8)	(14.9)	(44.6)	(75.0)

[a]Liver of a rat treated with phenobarbital (80 mg/kg body weight/day IP, once daily for 3 days). One to 1000 pg of total RNA extracted from 10-μm-thick sections by RNeasy Mini was subjected to one-step RT-PCR of GAPDH with the TaqMan probe detection system and CYP2B1 with the SYBR Green detection system.
[b]Relative expression (% of the level at 1000 pg of total RNA from unfixed cryosections). Values are expressed as mean ± SD.
[c]Values in parentheses represent the CV.
[d]Significantly different from the corresponding unfixed frozen section ($p<0.05$ by Student's t-test).

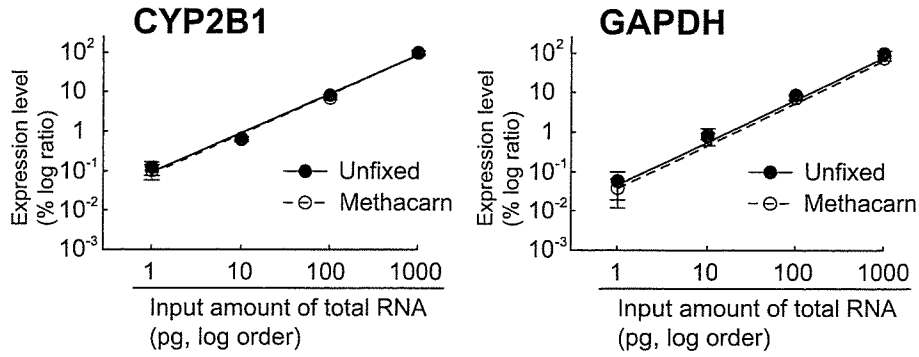

Figure 4 Linearity assessment of mRNA expression in the methacarn-fixed PET sections with the input amount of extracted total RNA in the range of 1–1000 pg. Expression levels of CYP2B1 and GAPDH were analyzed with one-step real-time RT-PCR. Relative expression levels were calculated when the values for the 1000 pg template RNA was accounted as 100% (mean ± SD; n=5). Pearson's correlation coefficients between the input amount of RNA and the expression of CYP2B1 or GAPDH were 0.997 and 0.990 in the unfixed frozen sections, and 0.991 and 0.982 in the methacarn-fixed PET sections.

rived from the MPOA of a male rat on postnatal day 10 (Figure 5). With the total RNA in the range of 5–45 ng, variability in the expression for each gene expressed as CV was mostly within 20%. In addition, high correlation of the expression levels to the input amount of total RNA was observed for all genes examined (0.972, 0.985, 0.965 and 0.985, respectively, for ERα, ERβ, GAT-1, and GAPDH).

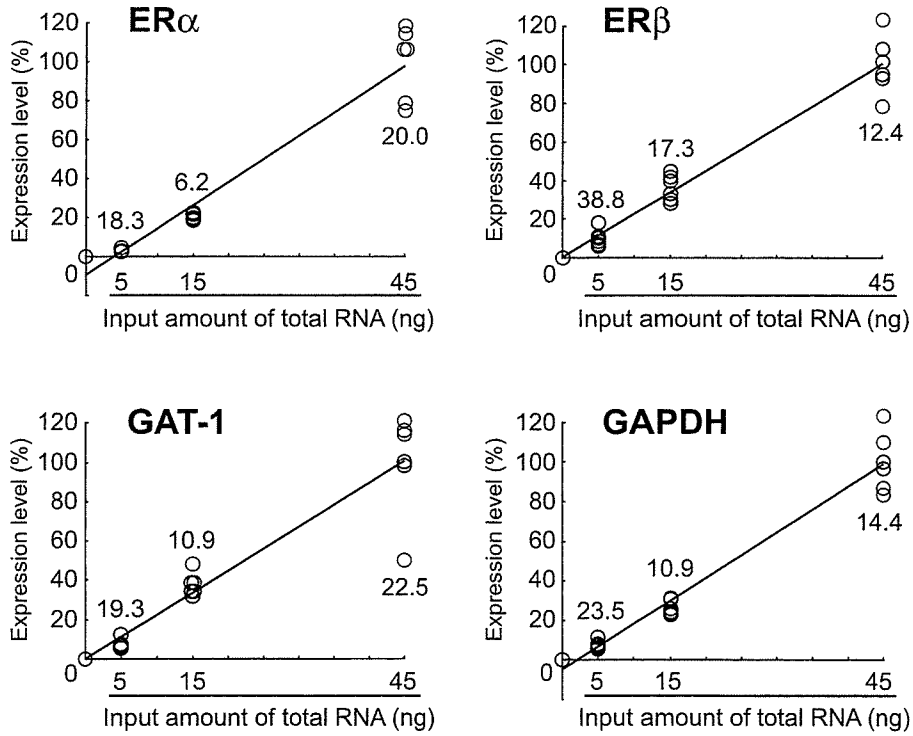

Figure 5 Variability of mRNA expression during the processes of RT and real-time PCR in the microdissected MPOA from methacarn-fixed, paraffin-embedded rat brain tissue. Total RNA extracted from microdissected specimens of MPOA from one male pup was divided to make triplicate samples for each of 5, 15, and 45 ng. RT was performed in a 20 μl of total volume. With 1 μl of RT product in duplicate, real-time PCR was performed for each gene utilizing the TaqMan probe detection system (ERα) or SYBR Green detection system (ERβ, GAT-1, and GAPDH). Relative expression levels were calculated when the values of the 45 ng template RNA was accounted as 100% (n=3). The values in the reverse transcriptase (−) mock RT product using 45 ng total RNA was used as those for zero template. Open circles represent expression levels in each sample. Numerical values in the graphs represent the CV of three samples in duplicate. Pearson's correlation coefficients between the input amount of total RNA and expression level of target gene were 0.972, 0.985, 0.965 and 0.985 for ERα, ERβ, GAT-1 and GAPDH, respectively.

Relative Abundance of mRNAs in the Hematoxylin-stained Sections

Table 3 shows the relative abundance of mRNA molecules retained in the hematoxylin-stained, methacarn-fixed PET sections in comparison with the unstained sections. RNA yields of unstained or hematoxylin-stained sections (ng/section, 10 μm in thickness) were 873 ± 276 (n=6), and 1136 ± 354 (n=5), respectively. Expression levels of CYP2B1 and GAPDH were examined with 1 or 10 ng of template total RNA. After hematoxylin staining, 0–20% reduction was observed in the relative abundance of amplifiable mRNAs for the genes, with statistical difference in CYP2B1 (p<0.05). The 1/10 reduction of the input amount of RNA (from 10 to 1 ng) reduced the expression levels of both CYP2B1 and GAPDH proportionally to ~1/10, irrespective of the tissue staining.

Gene Expression Analysis in the Microdissected MPOA of Rat Pups

Because sexual dimorphism in the expression of ERα in the developing rat MPOA has been demonstrated by IHC (Yokosuka et al. 1997), expression level of ERα mRNA was examined in the microdissected MPOA of rat pups at postnatal day 10 (Figure 6), along with the ERβ mRNA expression level, for which no substantial sexual dimorphism in the MPOA was found both by IHC and in situ hybridization (Orikasa et al. 2002). Expression of ERα mRNA in females was higher than that in males (Figure 6), even when the expression level was normalized to the GAPDH value. The ERβ mRNA expression level, on the other hand, did not differ between males and females. IHC of ERα in the brains at the same age demonstrated intense nuclear staining in the hypothalamic brain region (Figure 7A). Numbers of ERα-immunoreactive nuclei counted in the MPOA corresponding to the area used for mRNA expression analysis (600 × 1000 μm) were higher in females than in males (Figures 7A and 7B).

Table 3 Relative abundance of mRNAs in unstained and hematoxylin-stained, methacarn-fixed PET sections[a]

	No. of samples	Extracted total RNA (ng)	
		10	1
CYP2B1			
Unstained	6	100.0 ± 14.8[b]	100.0 ± 18.3 (9.0)[c]
Hematoxylin-stained	5	77.6 ± 5.1[d]	79.3 ± 6.5[d] (9.2)
GAPDH			
Unstained	6	100.0 ± 17.4	100.0 ± 18.1 (10.5)
Hematoxylin-stained	5	100.3 ± 17.1	85.0 ± 16.7 (8.9)

[a]Liver of a rat treated with phenobarbital (80 mg/kg body weight/day IP, once daily for 3 days). A 1- or 10-ng aliquot of total RNA extracted from 10-μm-thick sections by RNeasy Mini was subjected to one-step RT-PCR of GAPDH with TaqMan probe detection system and CYP2B1 with SYBR Green detection system.
[b]Expression level (%) relative to corresponding unstained sections. Values are mean ± SD.
[c]Values in parentheses represent (%) expression levels of corresponding tissue section with 10 ng input amount of RNA.
[d]Significantly different from the corresponding unstained section (p<0.05 by Student's t-test).

Cell Numbers Required for mRNA Expression

To determine the cell numbers required for quantitative measurement of mRNA expression in methacarn-fixed PET sections, hematoxylin-stained 10-μm-thick liver sections of a rat treated with 80 mg/kg PB were used and tissue areas up to 100 μm in radius were randomly microdissected from the mid-zonal areas of liver lobules. One-step real-time RT-PCR for CYP2B1 and GAPDH was performed. Table 4 shows the difference in the threshold cycle (C_T: fractional cycle number at which the fluorescent signal passes the fixed threshold) between the microdissected samples and standard samples, showing the lower limit within the dynamic range of amplification in each gene. For CYP2B1 expression, one or more circle tissues of 100 μm in radius, corresponding to >52 ± 3 liver cells (n=10), showed a C_T within the dynamic range of amplification. For GAPDH expression, most tissue-samples of more than 50 μm in radius showed a C_T within the dynamic range of amplification. Data variability between samples of identical tissue size was ex-

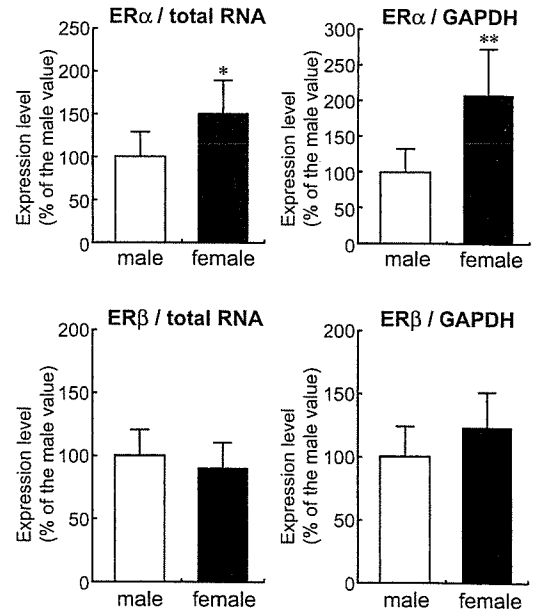

Figure 6 Measurement of mRNA expression levels of ERα and ERβ in the MPOA of male and female rat pups at postnatal day 10 using methacarn-fixed PET specimens. Numbers of animals examined were 5 for males and 6 for females. RT was performed with 24 ng of total RNA in a 20-μl total volume. With 1 μl of RT product, real-time PCR of each gene was performed. The values of ERα and ERβ were normalized for the amount of total RNA (left panels) or the expression level of GAPDH (right panels), and expressed as mean + SD. **, *: Significantly different from the male expression levels (*p<0.05, ** p<0.01 by Student's t-test).

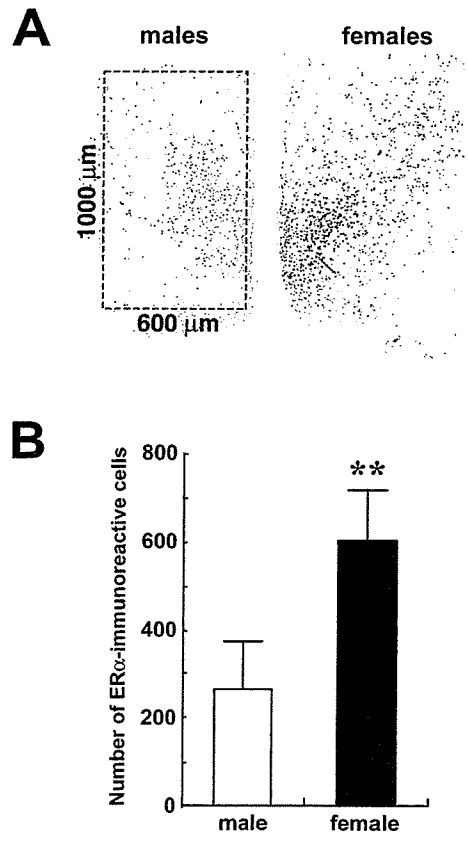

Figure 7 Sex difference of the ERα-immunoreactive cell population in the MPOA of rat pups at postnatal day 10. (**A**) Number of immunoreactive nuclei was counted in one MPOA (1000 × 600 μm) of one section in each animal. Left, male; right, female. (**B**) Mean numbers of immunoreactive cells in the MPOA (mean + SD; $n=3$ for both males and females). **: Significantly different from the male value ($p<0.01$ by Student's t-test).

pressed as CV for the "difference in C_T." With both genes, variability of data was decreased with an increase in the area of microdissected tissue, and less variable data were obtained with samples corresponding to the 208 cell/area. Variability between samples was greater with CYP2B1 compared with GAPDH.

Total RNA Yields in the Microdissected Tissue Areas

Table 5 shows RNA yields for microdissected unit areas of hematoxylin-stained rat liver PET sections. With increase in tissue size, RNA yield was proportionally increased. Because 1 ng/ml is the lower detection limit of RNA quantitation with RiboGreen fluorescent dye (manufacturer's instructions), in the rat liver a 250 × 250-μm area (corresponding to 104 cells) was the detection limit of RNA quantitation.

Discussion

Methacarn is an organic solvent fixative and therefore would not be expected to modify nucleotides or polypeptides as reported for crosslinking fixatives, such as formaldehyde (reviewed by Srinivasan et al. 2002). Previously, we have found that methacarn fixation followed by paraffin embedding does not affect the integrity of extracted total RNA, but results in halving of the RNA yield from unfixed frozen samples (Shibutani et al. 2000). However, we could here extract total RNA from methacarn-fixed rat liver sections with an efficiency equivalent to that with unfixed cryosections. Although we could not identify the reason for the observed difference between the previous and present studies, the tissue condition (tissue blocks in the previous study vs sectioned tissues in the present study), normalization of RNA yield (wet weight vs unit area), or extraction tool (RNASTAT-60 utilizing isopropanol precipitation for RNA isolation vs RNeasy Mini utilizing selective binding properties of silica gel-based membrane for RNA isolation) might have exerted an influence. We also observed only a small reduction in the relative abundance of amplifiable mRNAs retained in the methacarn-fixed PET sections compared with unfixed cryosections. Slight reduction of the integrity of extracted total RNA in the methacarn-fixed PET sections may be parallel to the results of the relative abundance of amplifiable mRNAs. On the other hand, methacarn itself does not appear to affect the quality of RNA molecules because fixation of fresh frozen sections for 10 min with this solution well preserved the integrity of total RNA in the present study. Considering the advantages in tissue handling during sectioning and after microdissection steps with PET specimens, as well as the disadvantages with unfixed frozen tissue in terms of tissue handling and instability of RNA molecules in sectioned specimens, methacarn fixation in combination with paraffin embedding has clear benefits for mRNA expression analysis of microdissected specimens.

Generally speaking, tissue staining with hematoxylin appears to affect both extraction efficiency and PCR amplification of genomic DNA (Murase et al. 2000; Serth et al. 2000), although in the present study the influence of brief staining with hematoxylin was marginal. Polynucleotides in tissue sections fixed with organic solvent fixatives, such as Carnoy's solution or methacarn, may be released into solution during IHC or ISH (Urieli-Shoval et al. 1992; Uneyama et al. 2002). However, methacarn-fixed PET sections could quickly be stained with hematoxylin in a period of 1–10 sec (Uneyama et al. 2002), and this might have contributed to the limited loss of extractable RNA after hematoxylin staining in the present study. We also observed only slight reduction (0–20%) in the relative abundance of amplifiable mRNAs after hematoxylin staining. We previously noted that staining with hematoxylin and eosin affected PCR of genomic DNA in methacarn-fixed PET sections, despite no deteriora-

Table 4 Difference in the C_T of real-time amplification in the microdissected samples from those of the lower limit of amplification in the standard samples[a]

	Tissue area (μm in radius)	Corresponding cell numbers[b]	No. of samples	Difference in C_T[c]	CV
Gene					
CYP2B1	100 × 4 pieces	208	6	3.9 ± 1.3[d]	33.3
	100 × 2 pieces	104	9	2.8 ± 2.0	71.4
	100 × 1 piece	52	8	1.6 ± 1.5	93.8
	50 × 1 piece	13	16	−1.7 ± 1.7	Not available
	30 × 1 piece	5	6	−2.1 ± 2.5	Not available
GAPDH	100 × 4 pieces	208	5	7.9 ± 0.4	5.1
	100 × 2 pieces	104	10	5.3 ± 1.5	28.3
	100 × 1 piece	52	9	1.9 ± 2.1	110.5
	50 × 1 piece	13	14	1.5 ± 1.9	126.7
	30 × 1 piece	5	5	−2.4 ± 1.3	Not available

[a]Liver tissue of a rat treated with PB at 80 mg/kg body weight/day for 3 days was used for both standard and microdissected samples. Unfixed frozen tissue was used for standard and hematoxylin-stained 10-μm-thick sections were subjected to analysis. With 5 μl of total RNA extracted by RNAqueous Micro, one-step RT-PCR was performed on GAPDH with the TaqMan probe detection system and CYP2B1 with the SYBR Green detection system.
[b]Cell numbers in each sample were calculated from the mean liver cell numbers in the circle area of 100 μm radius (52 ± 3; n=10).
[c]Values were calculated by subtracting the C_T of each sample from the C_T of the standard sample showing the lower limit of amplification. Expressed as mean ± SD.
[d]Amount of total RNA and its C_T (mean ± SD) of the standard sample at the lower limit of amplification within the dynamic range was respectively 0.4 pg and 32.4 ± 1.3 cycles for CYP2B1 (n=3), and 0.4 pg and 38.1 ± 0.9 cycles for GAPDH (n=4).

tion of the integrity and yield of extracted DNA (Uneyama et al. 2002). Hematoxylin has been reported to influence divalent cations (Mg^{2+}) that are important for maintaining Taq DNA polymerase activity (Chen et al. 1996), and this was reported to be apparent when manually dissected large tissue samples are subjected to PCR analysis (Burton et al. 1998; Murase et al. 2000). However, such an inhibitory effect might be negligible when microdissected small tissue specimens are analyzed (Ehrig et al. 2001). In line with the present study results, hematoxylin staining did not affect RT-PCR when microdissected small tissue specimens were analyzed in a previous study (Imamichi et al. 2001).

The cell number required for mRNA expression analysis in microdissected tissue specimens is primarily dependent on the expression level of the target genes of interest. In the case of cyclin D1 in primary tumor tissues, Specht et al. (2002) reported that transcripts could be measured in a minimum of 20 microdissected tumor cells from formalin-fixed PET specimens with an improved extraction protocol and the TaqMan PCR method in combination, but they also found 2000 cells to be suitable to obtain reproducible real-time PCR results. Although the expression values did not greatly vary (CV <20) from 100 pg of total RNA in the present experiment examining relative abundance of amplifiable mRNAs (Table 2), ~200 cells (corresponding to 2 ng based on the RNA yield data in Table 5) can be considered as a minimum for the practical expression analysis of mRNA species, judging from the very small variation of difference in C_T values of GAPDH gene with the corresponding tissue size (100 μm in radius × 4 pieces) reflecting homogeneity in the expression between samples as well as very small technical variation (Table 4). Expression levels of CYP2B1 varied between samples, even with a tissue area of 208 cells. With PB treatment, graded expression of CYP2B1 in the liver lobule occurs in the rat, with pronounced induction in the periportal region (Bühler et al. 1992). In the present study, midzonal areas of hepatic lobules were subjected to analysis, and therefore the variability of CYP2B1 expression in each sample might rather reflect a local event due to the graded expression profile of the transcript within this area.

In the present study, the concentration of total RNA was measured by RiboGreen fluorescent dye, with 1 ng as the lower detection limit in a 1-ml assay volume, and we could obtain ~1 ng of total RNA from 100 microdissected liver cells. If normalization of mRNA expression level to the input amount of total RNA is intended, a total of 3 ng or more (corresponding to >300 cells in a 10-μm-thick section of the rat liver)

Table 5 Total RNA yields in microdissected unit areas of methacarn-fixed rat liver PET sections[a]

Microdissected area[b]	No. of samples	RNA yield (ng/tissue)
1000 × 1000 μm (1669 cells)[c]	5	34.1 ± 5.81
500 × 500 μm (417 cells)	4	5.8 ± 2.89
250 × 250 μm (104 cells)	5	1.3 ± 0.16

[a]Liver of a rat treated with PB at 80 mg/kg body weight/day for 3 days. Total RNA (20 μl) extracted with RNAqueous-Micro was subjected to determination of RNA yield by RiboGreen RNA Quantitation kit.
[b]Tissue sections 10 μm thick were stained with hematoxylin before microdissection.
[c]Numbers of cells contained in each area were calculated from the mean cell numbers in the circle area of 100 μm radius as estimated in Table 4.

would be necessary for measurement of RNA concentration (1 ng) and after real-time RT-PCR of several genes (2 ng) under the present experimental conditions. If a fluorescence microplate reader is available, the total volume for assay of total RNA concentration could be minimized. As another normalization method, the expression level of a reference gene can be used. Housekeeping genes, such as GAPDH in the present study, are usually selected for this purpose. However, disadvantages with a single housekeeping gene were recently reported (Lee et al. 2002; Tricarico et al. 2002), and sexual dimorphism exists in GAPDH expression in several brain regions of developing rats (Perrot-Sinal et al. 2001). Sexual dimorphism of ERα expression in MPOA was apparent here, irrespective of the normalization method.

In conclusion, we have now demonstrated that methacarn-fixed PET allows practical mRNA expression analysis in microdissected areas with real-time RT-PCR after hematoxylin staining. Although recent studies have also demonstrated good performance of mRNA expression measurement with microdissected formalin-fixed PETs (Specht et al. 2001,2002), formaldehyde causes modification of nucleotides and therefore a high frequency of non-reproducible sequence alteration and amplification of only short fragments (reviewed by Srinivasan et al. 2002), suggesting limited utility for molecular analysis. Considering the availability for both DNAs and proteins in PET sections (Shibutani et al. 2000; Shibutani and Uneyama 2002; Uneyama et al. 2002), methacarn should prove to be a versatile tool for multipurpose analysis of target genes in specific cell populations. We are now applying methacarn for global gene expression analysis using a microarray technique with microdissected PET specimens. The question of how long molecules are retained intact in methacarn-fixed PET should now be addressed. Although we do not have data for archival tissues stored for several years/decades, mRNA levels could be measured with methacarn-fixed PET that had been prepared 6 months previously in the present study.

Acknowledgments

Supported in part by Health and Labor Sciences Research Grants (Research on Food and Chemical Safety) from the Ministry of Health, Labor and Welfare of Japan.

Literature Cited

Bühler R, Lindros KO, Nordling Å, Johansson I, Ingelman-Sundberg M (1992) Zonation of cytochrome P450 isozyme expression and induction in rat liver. Eur J Biochem 204:407–412

Burton MP, Schneider BG, Brown R, Escamilla-Ponce N, Gulley ML (1998) Comparison of histologic stains for use in PCR analysis of microdissected, paraffin-embedded tissues. Biotechniques 24:86–92

Chen JT, Lane MA, Clark DP (1996) Inhibitors of the polymerase chain reaction in Papanicolaou stain. Removal with a simple destaining procedure. Acta Cytol 40:873–877

Ehrig T, Abdulkadir SA, Dintzis SM, Milbrandt J, Watson MA (2001) Quantitative amplification of genomic DNA from histological tissue sections after staining with nuclear dyes and laser capture microdissection. J Mol Diagn 3:22–25

Emmert-Buck MR, Bonner RF, Smith PD, Chuaqui RF, Zhuang Z, Goldstein SR, Weiss RA, et al. (1996) Laser capture microdissection. Science 274:998–1001

Higuchi R, Dollinger G, Walsh PS, Griffith R (1992) Simultaneous amplification and detection of specific DNA sequences. Biotechnology 10:413–417

Higuchi R, Fockler C, Dollinger G, Watson R (1993) Kinetic PCR analysis: real-time monitoring of DNA amplification reactions. Biotechnology 11:1026–1030

Ikeda K, Monden T, Kanoh T, Tsujie M, Izawa H, Haba A, Ohnishi T, et al. (1998) Extraction and analysis of diagnostically useful proteins from formalin-fixed, paraffin-embedded tissue sections. J Histochem Cytochem 46:397–403

Imamichi Y, Lahr G, Wedlich D (2001) Laser-mediated microdissection of paraffin sections from Xenopus embryos allows detection of tissue-specific expressed mRNAs. Dev Genes Evol 211: 361–366

Kocarek TA, Kraniak JM, Reddy AB (1998) Regulation of rat hepatic cytochrome P450 expression by sterol biosynthesis inhibition: inhibitors of squalene synthase are potent inducers of CYP2B expression in primary cultured rat hepatocytes and rat liver. Mol Pharmacol 54:474–484

Lee PD, Sladek R, Greenwood CM, Hudson TJ (2002) Control genes and variability: absence of ubiquitous reference transcripts in diverse mammalian expression studies. Genome Res 12:292–297

Murase T, Inagaki H, Eimoto T (2000) Influence of histochemical and immunohistochemical stains on polymerase chain reaction. Mod Pathol 13:147–151

Orikasa C, Kondo Y, Hayashi S, McEwen BS, Sakuma Y (2002) Sexually dimorphic expression of estrogen receptor β in the anteroventral periventricular nucleus of the rat preoptic area: implication in luteinizing hormone surge. Proc Natl Acad Sci USA 99: 3306–3311

Perrot-Sinal TS, Davis AM, McCarthy MM (2001) Developmental sex differences in glutamic acid decarboxylase (GAD(65)) and the housekeeping gene, GAPDH. Brain Res 922:201–208

Puchtler H, Waldrop FS, Meloan SN, Terry MS, Conner HM (1970) Methacarn (methanol-Carnoy) fixation. Practical and theoretical considerations. Histochemie 21:97–116

Rhees RW, Shryne JE, Gorski RA (1990a) Onset of the hormone-sensitive perinatal period for sexual differentiation of the sexually dimorphic nucleus of the preoptic area in female rats. J Neurobiol 21:781–786

Rhees RW, Shryne JE, Gorski RA (1990b) Termination of the hormone-sensitive period for differentiation of the sexually dimorphic nucleus of the preoptic area in male and female rats. Dev Brain Res 52:17–23

Schütze K, Lahr G (1998) Identification of expressed genes by laser-mediated manipulation of single cells. Nature Biotechol 16:737–742

Serth J, Kuczyk MA, Paeslack U, Lichtinghagen R, Jonas U (2000) Quantitation of DNA extracted after micropreparation of cells from frozen and formalin-fixed tissue sections. Am J Pathol 156: 1189–1196

Shibutani M, Uneyama C, Miyazaki K, Toyoda K, Hirose M (2000) Methacarn fixation: a novel tool for analysis of gene expressions in paraffin-embedded tissue specimens. Lab Invest 80:199–208

Shibutani M, Uneyama C (2002) Methacarn: a fixation tool for multipurpose genetic analysis from paraffin-embedded tissues. In Conn PM, ed. Laser Capture Microscopy and Microdissection. Methods Enzymol 356. London, Academic Press, 114–125

Specht K, Kremer M, Muller U, Dirnhofer S, Rosemann M, Hofler H, Quintanilla-Martinez L, Fend F (2002) Identification of cyclin D1 mRNA overexpression in B-cell neoplasias by real-time reverse transcription-PCR of microdissected paraffin sections. Clin Cancer Res 8:2902–2911

Specht K, Richter T, Muller U, Walch A, Werner M, Hofler H (2001) Quantitative gene expression analysis in microdissected archival formalin-fixed and paraffin-embedded tumor tissue. Am J Pathol 158:419–429

Srinivasan M, Sedmak D, Jewell S (2002) Effect of fixatives and tissue processing on the content and integrity of nucleic acids. Am J Pathol 161:1961–1971

Tricarico C, Pinzani P, Bianchi S, Paglierani M, Distante V, Pazzagli M, Bustin SA, et al. (2002) Quantitative real-time reverse transcription polymerase chain reaction: normalization to rRNA or single housekeeping genes is inappropriate for human tissue biopsies. Anal Biochem 309:293–300

Uneyama C, Shibutani M, Masutomi N, Takagi H, Hirose M (2002) Methacarn fixation for genomic DNA analysis in microdissected, paraffin-embedded tissue specimens. J Histochem Cytochem 50:1237–1245

Urieli-Shoval S, Meek RL, Hanson RH, Ferguson M, Gordon D, Benditt EP (1992) Preservation of RNA for in situ hybridization: Carnoy's versus formaldehyde fixation. J Histochem Cytochem 40:1879–1885

Yokosuka M, Okamura H, Hayashi S (1997) Postnatal development and sex difference in neurons containing estrogen receptor-alpha immunoreactivity in the preoptic brain, the diencephalon, and the amygdala in the rat. J Comp Neurol 389:81–93

Available online at www.sciencedirect.com
SCIENCE DIRECT®
Analytical Biochemistry 351 (2006) 36–43
ANALYTICAL BIOCHEMISTRY
www.elsevier.com/locate/yabio

Methacarn fixation—effects of tissue processing and storage conditions on detection of mRNAs and proteins in paraffin-embedded tissues

Kyoung-Youl Lee [1], Makoto Shibutani *, Kaoru Inoue, Keiko Kuroiwa, Mami U, Gye-Hyeong Woo, Masao Hirose

Division of Pathology, National Institute of Health Sciences, 1-18-1 Kamiyoga, Setagaya-ku, Tokyo 158-8501, Japan

Received 29 September 2005
Available online 8 February 2006

Abstract

In this study, we examined suitable conditions for tissue fixation with methacarn and ethanol dehydration and storage of paraffin-embedded tissues (PETs) on gene expression analysis. With fixation and dehydration of rat liver tissues for up to 16 h (overnight) and 1 week, respectively, at 4 °C, integrity of extracted total RNAs and polypeptides did not vary, the former integrity being constantly lower than that with unfixed frozen tissue, while protein yield was slightly reduced with increasing dehydration. Retained expression levels of mRNAs and proteins were mostly unaffected by the period of fixation but slightly fluctuated with the length of dehydration. When PETs were stored for up to 12 months, integrity of both total RNAs and polypeptides was retained at 4 °C but reduced at room temperature. Reduced expression levels of mRNAs and proteins were also noted by storage at room temperature after 12 and 3 months, respectively. However, neither tissue processing nor storage affected variability in either mRNA or protein levels among samples. Thus, the results suggest that, for gene expression analysis, tissues can be fixed with methacarn and dehydrated for at least 1 day and 1 week, respectively, and PETs can be stored for at least 12 months, but a temperature of 4 °C is preferable.

Keywords: Methacarn; Molecular integrity; Paraffin-embedded tissue; Expression analysis

Molecular analysis of pathological specimens has provided insights into mechanisms underlying disease, facilitating development of diagnostic/therapeutic agents. To elucidate pathological processes in target cells involving alterations in cellular functions, application of microdissection techniques allows high performance even with a complex tissue architecture [1–3]. For molecular analysis, tissue samples should preferably be kept biochemically unmodified, and therefore unfixed frozen tissue (UFT)[2] has become the gold standard for analysis by microdissection and microbiochemical techniques. However, as compared with paraffin-embedded tissues (PETs), UFTs are inconvenient with regard to storage and skills required for preparation and subsequent microdissection itself. Therefore tissue embedding after fixation is preferable if extraction of molecules with high quality and yield can be guaranteed.

We have recently found that methacarn, an organic-solvent-based noncross-linking fixative [4], retains advantages for analysis of expression levels of mRNAs and proteins and for analysis of mutations of target genes in microdissected tissue samples from PETs, with performance close to that possible with UFTs [5–10]. Another group confirmed the suitability of methacarn among a series of fixatives for differential mRNA expression analysis using microdissected PET specimens [11]. For these earlier studies, tissue fixation with methacarn and ethanol dehydration was performed at 4 °C, default time settings for each step were

* Corresponding author. Fax: +81 3 3700 1425.
E-mail address: shibutan@nihs.go.jp (M. Shibutani).
[1] Present address: Department of Anatomy and Neurobiology, Faculty of Medicine, Kagawa University, 1750-1 Miki-cho, Kita-gun, Kagawa 761-0793, Japan.
[2] *Abbreviations used:* UFT, unfixed frozen tissue; PET, paraffin-embedded tissue; PB, sodium phenobarbital; PCNA, proliferating cell nuclear antigen; EGFR, epidermal growth factor receptor.

0003-2697/$ - see front matter © 2006 Elsevier Inc. All rights reserved.
doi:10.1016/j.ab.2006.01.032

empirically determined by selecting the minimal time period for each step (1 or 2 h for fixation and three times 1 h for dehydration under gentle agitation), and analyses of molecules were performed usually within 1 month after paraffin embedding. However, we did not examine the effects of fixation and following dehydration periods or the storage time and temperature after paraffin embedding.

Determination of a suitable range for lengths of fixation/dehydration steps is very important for practical molecular analysis using methacarn if large numbers of tissue samples are to be analyzed, such as in the case of animal experiments requiring time-consuming autopsy. Furthermore, conditions for long-term storage of PETs for effective molecular analysis need to be optimized. The present study was therefore performed using methacarn-fixed and paraffin-embedded rat liver tissues from one animal with differing periods of processing and storage, focusing on the integrity of extracted molecules and the relative expression levels in sections.

Materials and methods

Chemicals and experimental animals

Sodium phenobarbital (PB) was purchased from Wako Pure Chemical Industries (Osaka, Japan). A 5-week-old CD (SD)IGS male rat from Charles River Japan Inc. (Atsugi, Japan) was maintained in an air-conditioned animal room (temperature 24 ± 1 °C, relative humidity 55 ± 5%) with a 12-h light/dark cycle and allowed ad libitum access to tap water and feed, CRF-1 (Oriental Yeast Co. Ltd., Tokyo, Japan). After 1-week acclimation, the rat was intraperitoneally injected with PB at 80 mg/kg body weight, once daily for 3 days. One day (24 h) after the last injection, the animal was killed by exsanguination from the abdominal aorta under deep anesthesia, and then the liver was removed for tissue processing. The dose was selected according to the PB-specific enzyme induction protocol described by Kocarek et al. [12], and the animal protocol was reviewed and approved by the Animal Care and Use Committee of the National Institute of Health Sciences, Japan.

Tissue preparation and storage

From the center portion of the left lobe, tissue blocks sized 5 × 5 × 3 mm were excised and subjected either to embedding in Tissue-Tek 4583 OCT compound (Sakura Finetek Japan, Tokyo, Japan) or to immersing in methacarn for tissue fixation. Methacarn solution consisting of 60% (vol/vol) absolute methanol, 30% chloroform, and 10% glacial acetic acid was freshly prepared and stored at 4 °C before fixation [5,7,9]. UFTs were quickly frozen in ethanol/dry ice and stored at −80 °C until sectioning on the next day after embedding. To examine the effects of length of time of tissue processing (Experiment 1), fixation with methacarn and subsequent dehydration with 99.5% ethanol were performed for 2 and 16 h (overnight), 5 and 16 h, 16 and 16 h, or 2 h and 1 week at 4 °C in a refrigerator. Tissue blocks were dehydrated twice in fresh ethanol solution for 1 h and then for 16 h (overnight) or 1 week. They were then paraffin embedded as described previously [9], and tissue sectioning was performed within 1 week after paraffin embedding. To examine PET storage conditions (Experiment 2), 2 h-fixed overnight-dehydrated tissues were stored for 1 month at 4 °C or 3 or 12 months either at 4 °C in a refrigerator or at room temperature in a laboratory. Both UFTs and PETs were sectioned at 10 μm and a total of 20 sections per block were collected in 1.5-ml microtubes for storage at −80 °C until extraction of molecules.

RNA analysis

Methacarn-fixed PET sections stored at −80 °C were subjected to deparaffinization with xylene three times for 5 min, immersed in 100% ethanol three times for 5 min, and immediately processed for RNA extraction using an RNeasy Mini kit (Qiagen GmbH, Hilden, Germany) according to the manufacturer's protocol. For UFT sections stored at −80 °C, total RNAs were immediately extracted after removal from the deep freezer. The final elution volume was set at 30 μl and contaminating genomic DNA was digested with DNase I (Ambion, Austin, TX) according to the manufacturer's protocol. For quantitation of RNA yield, 1 μl of isolated RNA was labeled with a RiboGreen RNA Quantitation kit (Molecular Probes, Eugene, OR) and concentrations were estimated with a fluorescence spectrophotometer F2500 (Hitachi Co. Ltd., Tokyo, Japan) in 1 ml of total volume with water [5]. To examine the integrity of 18S and 28S ribosomal RNAs in the extracted total RNAs, 1 μg from each sample was loaded onto a 1.0% agarose gel and visualized with ethidium bromide. The integrity was also examined by measuring the 28S/18S ribosomal RNA ratio with an RNA 6000 Nano LabChip kit (Agilent Technologies, Mountain View, CA) and RNA ladders (Ambion) in an Agilent 2100 bioanalyzer according to the manufacturer's directions.

For measurement of relative mRNA expression levels, the following four mRNA species were selected: cytochrome P450 (CYP) 2B1 (GenBank/EMBL Data Bank, Accession No. M37134), glyceraldehyde-3-phosphate dehydrogenase (GAPDH; Accession No. M17701), solute carrier family 34A2 (slc34a2; Accession No. NM_053380.1), and syntaxin 6 (stx6; Accession No. NM_031665.1). CYP2B1 is a gene that is known to show strong induction in the liver by PB treatment of rats [9], and GAPDH is a representative housekeeping gene. Slc34a2 and stx6 were found to show specific expression changes by microarray analysis at the tumor promotion stage in the experimental hepatocarcinogenesis study previously performed in our laboratory using rats, and their expression levels relative to that of GAPDH were found to be rather minor by real-time RT-PCR analysis (data not shown). For measurement of GAPDH and CYP2B1 mRNA levels, one-step real-time RT-PCR with the SYBR Green detection system was performed using the

ABI PRISM 7000 Sequence Detection System (Applied Biosystems Japan, Tokyo, Japan) in a 50-μl total reaction volume including 50 ng of total RNA, 300 nM each forward and reverse primers, 12.5 U Multiscribe Reverse Transcriptase, 10 U RNase Inhibitor, and 25 μl SYBR Green PCR Master Mix, according to the manufacturer's protocol (all reagents were purchased from Applied Biosystems Japan). Primer sets for both genes were identical with those used in our previous study [9]. Cycle parameters in this system were as follows: single step of 48 °C for 30 min, single step of 95 °C for 10 min, and 50 cycles of 95 °C for 15 s followed by 60 °C for 1 min. As for measurement of mRNA levels of slc34a2 and stx6, two-step real-time RT-PCR with the TaqMan probe detection system was performed. Gene-specific primers and the corresponding TaqMan MGB probes (6-FAM-dye-labeled) were derived from TaqMan Gene Expression Assays (Applied Biosystems Japan Ltd.). Reverse transcription was performed using 1 μg of total RNA with a High-capacity cDNA Archive Kit (Applied Biosystems Japan Ltd.) in a 100-μl total reaction volume. Real-time PCR was performed in a 50-μl reaction volume using the TaqMan probe detection system with 25 μl of TaqMan Universal PCR Master Mix (Applied Biosystems Japan Ltd.) and 2.5 μl each of target primer mix and reverse transcription product corresponding to 50 ng total RNA. Cycle parameters with this system were single step of 50 °C for 2 min, and initial activation at 95 °C for 10 min, and 50 cycles of 15 s at 95 °C and 60 s at 60 °C. Among real-time PCR methods, SYBR Green and TaqMan assays are known to produce comparable dynamic range and sensitivity [13]. For quantitation of expression data, a standard curve method was applied using the total RNA from UFTs as a standard sample.

Protein analysis

Deparaffinized sections were treated with 10% trichloroacetic acid in saline at 4 °C for 15 min. After brief centrifugation, pellets were washed once with ice-cold saline and then sonicated and solubilized in 200 μl of 2× sodium dodecyl sulfate (SDS) gel-loading buffer excluding bromophenol blue. Protein concentrations were estimated using a NanoOrange Protein Quantitation Kit (Molecular Probes) and a fluorescence spectrophotometer [5]. After adjusting the protein concentration with 1× SDS gel-loading buffer including bromophenol blue, samples were heat-denatured at 80 °C for 30 min in the presence of 10% (v/v) β-mercaptoethanol and applied to 10% SDS polyacrylamide gel electrophoresis. For analysis of protein integrity, 20 μg of each protein extract was loaded, and resolved polypeptides were visualized after staining with 2.5% Coomassie brilliant blue. For Western blot analysis, resolved polypeptides were transferred to a polyvinylidine difluoride membrane (Millipore, Billerica, MA). Expression of three molecules with different functions and subcellular localizations were examined. After blocking with 0.2% casein, blots were incubated with either mouse monoclonal anti-β-actin (clone AC-15; Sigma; 20,000× in dilution), proliferating cell nuclear antigen (PCNA; clone PC10; Upstate, Charlottesville, VA; 1000× in dilution), or epidermal growth factor receptor (EGFR; clone 6F1; Medical and Biological Laboratories Co., Ltd., Nagoya, Japan; 300× in dilution) antibodies. Amounts of protein extract applied were 1 μg for β-actin, 5 μg for PCNA, and 15 μg for EGFR. As the secondary antibody, horseradish peroxidase-conjugated goat anti-mouse immunoglobulin (DakoCytomation Co., Ltd., Kyoto, Japan; 2000× in dilution) was used, and protein signals were detected with the ECL Western Blotting Detection System (Amersham Biosciences Corp., Piscataway, NJ). Relative protein levels of β-actin, PCNA, and EGFR were estimated by analyzing the band intensities using ONE-D/ZERO-Dscan Quantitative Gel and Blot Analysis software (Scanalytics, Inc., Fairfax, VA).

Statistical analysis

Comparison of 28S/18S ribosomal RNA ratios, yields of total RNA and protein, and expression levels of mRNA and protein retained in the tissues was performed with Student's *t* test when the variance was indicated to be homogeneous among groups using the test for equal variance. If a significant difference in the variance was observed, Welch's *t* test was performed. Comparison was first made between UFT and each PET preparation. In Experiment 1, comparisons were further performed between samples subjected to 2-h fixation/overnight dehydration or other fixation/dehydration conditions. Similar comparisons were also performed for Experiment 2. Variability was expressed as coefficient of variation (CV).

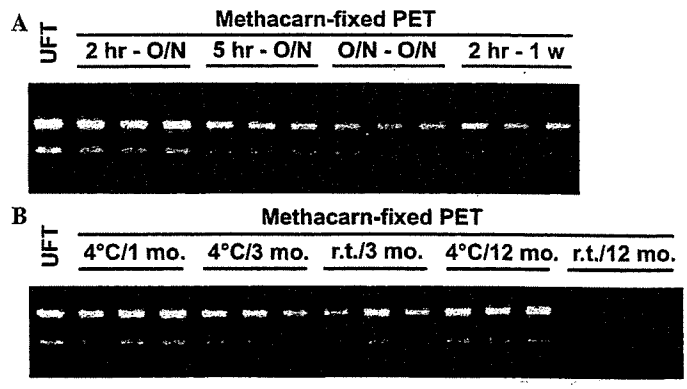

Fig. 1. Integrity of total RNAs extracted from methacarn-fixed rat liver PETs under different conditions of tissue processing or storage. One microgram of total RNA was applied to a 1% agarose gel and visualized with ethidium bromide. (A) Effects of period of tissue processing (Experiment 1): UFT, unfixed frozen tissue; 2 hr-O/N, samples fixed for 2 h followed by overnight dehydration; 5 hr-O/N, samples fixed for 5 h and dehydrated overnight; O/N-O/N, samples fixed overnight and then dehydrated overnight; 2 hr-1 w, samples fixed for 2 h and dehydrated for one week. (B) Storage effects of PETs with regard to period and temperature (Experiment 2): UFT, unfixed frozen tissue; 4 °C/1 mo., PETs stored for 1 month at 4 °C; 4 °C/3 mo., PETs stored for 3 months at 4 °C; r.t./3 mo., PETs stored for 3 months at room temperature; 4 °C/12 mo., PETs stored for 12 months at 4 °C; r.t./12 mo., PETs stored for 12 months at room temperature.

Results

Integrity and yield of total RNAs

In Experiment 1, integrity of total RNAs as judged by visual intensities for 18S and 28S ribosomal RNAs in agarose gel was not appreciably changed by the period of fixation up to overnight and dehydration up to 1 week (Fig. 1A). On measurement of the 28S/18S ribosomal RNA ratio, the integrity of total RNA was significantly reduced in methacarn-fixed PET sections compared with UFT sections (Table 1). The ribosomal RNA ratio remained unchanged from that of the 2-h fixed/overnight dehydrated case, although a tendency for reduction was observed in cases fixed for 5 h or overnight. Relative yields of total RNA per unit area were similar for all cases (Fig. 2A).

Table 1
28S/18S rRNA ratio of extracted total RNA in methacarn-fixed PETs under the different conditions for tissue processing or storage

Tissue condition	No. of samples	rRNA ratio [28S/18S][c]
Unfixed frozen	9	1.70 ± 0.45
Methacarn-fixed paraffin-embedded		
Fixation/dehydration[a]		
2 h/overnight	3	0.83 ± 0.07*
5 h/overnight	3	0.58 ± 0.04**
Overnight/overnight	3	0.62 ± 0.14**
2 h/1 week	3	0.70 ± 0.07**
Temperature/duration of storage[b]		
4 °C/1 month	6	0.75 ± 0.06**
4 °C/3 months	6	0.79 ± 0.09**
r.t./3 months	6	0.59 ± 0.14**
4 °C/12 months	6	0.66 ± 0.05**
r.t./12 months	6	Unmeasurable

*,**Significantly different from the unfixed frozen samples (*$p < 0.05$, **$p < 0.01$).

[a] Examination of the effect of time length for tissue processing (Experiment 1). Fixation and ethanol dehydration were performed at 4 °C. After dehydration, tissue blocks were paraffin embedded as described under Materials and methods. Already prepared PETs were stored at 4 °C until all of the tissues were processed for embedding.

[b] Examination of the effect of tissue storage with regard to the period and its temperature (Experiment 2). Fixation and ethanol dehydration were performed at 4 °C for 2 h and overnight, respectively. At the end of storage, tissue sections were prepared and stored at −80 °C until analysis.

[c] Data are expressed as mean ± SD.

In Experiment 2, when the visual integrity was compared among PET samples with different storage conditions, apparent reduction of both 18S and 28S ribosomal RNA bands was noted in samples stored for 12 months at room temperature (Fig. 1B), and this reduction resulted in the ribosomal RNA ratio being unmeasurable (Table 1). Although a nonsignificant reduction in the ribosomal RNA ratio was noted in PET samples stored for 3 months at room temperature as compared with those stored for 1 month at 4 °C, other PET storage conditions did not change the integrity of total RNA extracted (Fig. 1B, Table 1). Relative yields of total RNA per unit area were similar between the 1-month-stored case at 4 °C and each of the other cases (Fig. 2B).

Levels of mRNAs retained in PETs

On measurement of mRNA levels in PETs, mean threshold cycle (C_T: fractional cycle number at which the fluorescent signal passes the fixed threshold) of each gene was measured under the same input amount of total RNA using representative PET samples, i.e., 2-h-fixed/overnight-dehydrated samples in Experiment 1 and 1-month-stored samples at 4 °C in Experiment 2 (Table 2). As expected, C_T values of both GAPDH and PB-induced CYP2B1 were much smaller than those of slc34a2 and stx6, with ≥ 10-cycle differences simply reflecting ≥ 1000-fold expression differences. Judging from C_T values, relative quantity of transcripts was estimated to be in the order of CYP2B1 > GAPDH ≫ slc34a2 > stx6.

In Experiment 1, the GAPDH mRNA level retained in PETs was reduced in tissues dehydrated for 1 week to 62.2% of the 2-h-fixed/overnight-dehydrated case, but period of fixation did not affect the mRNA level (Fig. 3A). CYP2B1 mRNA levels were not apparently changed by the tissue-processing conditions. With regard to slc34a2, slight reduction of mRNA level was observed by 5-h fixation/overnight dehydration and 2-h fixation/1-week dehydration. Stx6 mRNA levels were not apparently changed irrespective of the fixation/dehydration conditions. With mRNA species examined, CV values ranged mostly within 20%, except for that of slc34a2 by overnight fixation being 40.0%.

In Experiment 2, retention of mRNAs in PETs was affected by storage for 12 months at room temperature, with reduction

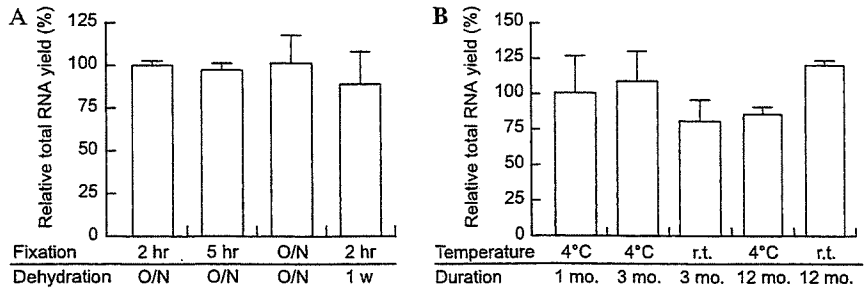

Fig. 2. Relative yields of total RNA in methacarn-fixed PETs under the different conditions of tissue processing or storage. (A) Experiment 1 ($n = 3$ for each condition). (B) Experiment 2 ($n = 6$ for each condition). Data are expressed as mean ± SD. Sample conditions were as for Fig. 1.